WADC TECHNICAL REPORT 54-402

CREEP BUCKLING OF COLUMNS

D. Rosenthal
D. Hasanovitsh

University of California

September 1954

Materials Laboratory
Contract No. AF 33(616)-379
RDO No. 614-13

Wright Air Development Center
Air Research and Development Command
United States Air Force
Wright-Patterson Air Force Base, Ohio

Carpenter Litho & Prtg. Co., Springfield, O.
300 - 21 December 1954

FOREWORD

This report was prepared by the University of California under USAF Contract No. AF 33(616)-379. The contract was initiated under Research and Development Order No. 614-13 M-A, "Design and Evaluation Data for Structural Metals", and was administered under the direction of the Materials Laboratory, Directorate of Research, Wright Air Development Center, with Mr. E. L. Horne acting as project engineer. D. Rosenthal directed and was technically responsible for the research described in this report.

ABSTRACT

An upper and lower bound to the exact solution of creep buckling has been evolved. In both cases time-deflection curves are computed using isochronous curves which are cross plotted from creep tension data. In addition to the usual assumptions of the beam theory the solution is based on the assumption that the variation of stress in the cross section can be approximated by a parabola in terms of the position in the plane of bending. Under these assumptions the method of solution is quite general and applicable to prismatic columns of any type and initial eccentricity. Comparison with experimental data on Stabilized 24S Aluminum Alloy suggests that the upper bound is a closer approximation to the solution than the lower one. There is also an indication that for moderately crooked columns subjected to high average stress the tangent modulus to the isochronous curve at the average stress level would provide a closer lower bound than the one given by the theory. The deflection at a given time could then be determined directly from the isochronous curve at this time. However, the justification for this procedure could not be established theoretically and it must come from the experiment.

An attempt to extend the theory to columns with high slenderness ratio shows that the solution depends critically on the initial eccentricity, a result which is in qualitative agreement with the experiment.

The investigation shows a need for further work, both experimental and theoretical. In particular, there is a need for duplicate tests to determine the scatter of experimental data.

PUBLICATION REVIEW

This report has been reviewed and is approved.

FOR THE COMMANDER:

M. R. WHITMORE
Technical Director
Materials Laboratory
Directorate of Research

TABLE OF CONTENTS

LIST OF FIGURES

NOTATIONS

Refer to Figures 1a and b

P - load on the column

l - length of column

z - distance of cross section from upper end

h - height of the cross sectional area

y - distance of fiber from the centroidal axis

μ - initial deflection (under no load) assumed to be a sinusoid

η_t, η_t^* - additional deflection under load at time t

η_t'' - curvature under load at time t

a - maximum initial deflection, or eccentricity

a_t - additional maximum deflection at time t

A - cross sectional area

S - static moment about x axis

I - moment of inertia about x axis

J - moment of third order about x axis, $J = \int y^3 dA$

r - radius of gyration,

l/r - slenderness ratio

r_c - core radius, $r_c = 2r^2/h$

s - S/A

e - initial eccentricity nondimensional, $e = \frac{a}{r_c}$

w_t - maximum deflection under load, nondimensional, $w_t = \frac{a_t}{r_c}$

σ - stress

ϵ - strain

σ_t - stress at the centroid at time t for $z = l/2$

$\Delta\sigma_t^*, \Delta\sigma_t$ - correction to σ_t, $\Delta\sigma_t = \sigma_t - \sigma_{t-1}$

$\Delta_t\sigma$ - stress difference between the inner and outer fiber at time t for $z = l/2$

$\Delta_t\epsilon, \Delta_t'\epsilon$ - strain difference corresponding to $\Delta_t\sigma$

E_t, E_t^* - tangent modulus at the centroid at time t

E_r - reduced tangent modulus, $E_r = \frac{E_0 + E_t}{2}$

ΔE_t - correction to E_t at time t

G_t - modulus of curvature at time t, $G_t = dE_t/d\epsilon$

P_t, P_t^* - Euler's load at time t, $P_t = \pi^2 E_t I/l^2$

p_t - ratio, $p_t = P_t/P$

ΔP_t - correction to P_t at time t

$P_t' = P_t + \Delta P_t$

$\sigma_{cr} = \pi^2 E_0 / (l/r)^2$

$\zeta = \pi z / l$

$\phi = \eta / a$

$\phi'' = d^2\phi / d\zeta^2$

$f = \phi_{max}$, for $\zeta = \pi/2$

$\omega = 2Pl^2 / \pi^2 (E_0 + E_t) I$

$\alpha = 2GJa\pi^2 / (E_0 + E_t) I l^2$

$\gamma_t = 2(E_0 - E_t) l^2 s / G_t \pi^2 r^2 a_t$

k - fraction

β - fraction

INTRODUCTION

The Problem

Metal parts subjected to high temperature service deform with time even though the applied load remains constant. The design criteria must therefore include time in the stress strain relationship of the material at a specified temperature. The basic information is generally provided in the form of strain-time data under uniaxial tension in which the load, or less frequently the stress, is kept constant. The problem consists of utilizing the above data in design for types of loading in which the stress no longer remains constant but changes in accordance with imposed boundary conditions. In this respect the behavior of columns subjected to axial compression is of particular importance because of what we may term as danger of collapse. Since the deflection is a monotonic and continuous function of time, there is no real critical buckling in creep. However, the column may start to deflect at an ever increasing rate at a time when a companion tensile specimen subjected to the same initial stress deforms at a constant, or even decreasing, rate.

This time may be designated conveniently as "collapse" time. Alternately, the designer may wish to know the time it takes the column to reach a certain specified value of deflection. This criterion is much easier to determine and it will be used in the present report for convenience. In both cases the problem is reduced to the computation of time-deflection curves under given initial conditions of loading.

Equations of State

An exact solution of the creep buckling problem is hardly possible in the present state of knowledge of creep phenomena in metals. If creep data under constant stress are to be used in cases where the stress varies, then a more general relationship between stress, strain, and time must be available at a specified temperature. The problem would have been a relatively easy one if the changes of strain depended only on the stress level and time, and not on the path and sign of stress. A simple cross plot of data would then provide the necessary relationship. This procedure is known to be incorrect. There is no unique equation, the so-called equation of state, between stress, strain, and time. However, as shown by Carlson (1)* the above relationship provides a lower bound for the solution of creep buckling.

An alternate procedure, which is more in accordance with recent tests, (2) is to consider separately the time free and the time dependent component of strain. The first component is considered to be path independent, but in the second term only its rate is taken as being path independent. This procedure has been suggested by Shanley (3) and it has been applied by Higgins (4) and Libove (5). In the present work it has been adopted for the purpose of finding an upper bound.

In a less general form similar procedures have been followed by Hoff (6), Kempner (7), Rosenthal and Baer (8), and others. That rate of straining may not be path independent has been clearly indicated by Orowan (9) and Dorn and coworkers (10). It may be some time before the path dependence of creep is fully understood, let alone formulated. In view of this situation

---

* Figures refer to appended Bibliography.

any analytical expression of the basic creep law at present can be only tentative and approximate.

Previous Methods of Solutions

Aside from the lack of a valid creep law the exact solution of the creep buckling problem is met with considerable mathematical difficulties. To avoid these difficulties approximate solutions are being sought through appropriate assumptions and simplifications. Even so, the mathematical labor involved in many methods in far from negligible. Most of the methods are applicable only to an idealized column and are based on a particular analytical form of the basic creep law. Very few have been checked experimentally. In view of this situation there seems to be some merit in the attempts which seek to obtain experimental verifications through the use of actual creep data and real columns, even at the expense of mathematical rigor. Such attempts have been made by Carlson (1), and Higgins (4). In both cases graphical methods of solutions were used. As mentioned previously Carlson's method was aimed at obtaining a lower bound. Higgins attempted a closer solution but got also a lower value. From the nature of the approximations made it is hard to predict whether his solution will fall on the lower or upper side of the exact solution. For the purpose of future computations it would seem however desirable to know beforehand on what side of the true solution the approximation is. Also the method is rather lengthy and it does not lend itself readily to generalization.

Present Method of Solution

The distinctive feature of the present method of solution is that it seeks to obtain an upper and lower bound to the solution rather than the exact solution.

Such an approach appears justified on at least three counts:

1. The correct stress-strain-time relationship is not known at present.
2. Even though such a relationship were available, its practical use would be severly hampered by mathematical difficulties; simplifying assumptions would have to be made subject to experimental verifications.
3. Because of the time element small and accidental changes in the initial conditions are likely to cause a large scatter of experimental data with the result that statistical bounds rather than a definite value would have to be assigned to these data. This at present is mere speculation since results of duplicate tests are not available.

As in the two aforementioned methods by Higgins and Carlson, actual creep tension data are cross plotted to yield isochronous stress-strain curves. However, the graphical method of solution is replaced here by an analytical one. To this end, relevant portions of the isochronous curves are approximated by segments of parabola. This approximation happened to fit the actual data of the Stabilized 24S Aluminum Alloy (used here for the purpose of experimental check) rather closely over large ranges of strains. However, it will appear later that a less close approximation would not have altered the final results substantially. In addition, not only is the analytical solution more rapid than the graphical one, but it can be put in a non - dimensional form. Thus the results can be applied to any type of prismatic column.

Section 1

BASIC RELATIONS

Assumptions and Limitations

1. The usual approximations of the beam theory are valid, viz., plane sections remain plane and second derivative of deflection can be substituted for curvature.

2. Changes of dimensions are small and can be neglected in computation.

3. Creep tension data are applicable to compressive loads.

4. The variation of stress in the cross section is at all times small compared to the average stress to justify a second order (parabolic) approximation to the actual stress distribution in the cross section. The limits of validity of this approximation are discussed subsequently.

5. The level of average stress is sufficiently high to cause at all times creep in all fibers of the cross section. Cases in which this condition is not satisfied will be considered separately in Section 5.

6. The present discussion is limited to cross sections symmetrical about the axis of minimum moment of inertia. The extension to other sections can be considered as a particular case of the problem discussed in Section 5.

Fundamental Equations

The first assumption leads to the usual compatibility equation for bending. If R is the radius of curvature, then the strain variation at

point y of the cross section is (see Figure 1a and b),

$$\Delta\epsilon = \epsilon - \epsilon_c = y/R = y\eta^* \tag{1.1}$$

By virtue of equation (1.1) assumption four can be formulated in terms of strains as follows

$$\sigma - \sigma_c = E_c(\epsilon - \epsilon_c) - G(\epsilon - \epsilon_c)^2 \tag{1.2}$$

Here σ_c and ϵ_c refer to the centroid, but may equally well refer to any point of the cross section, and E_c and G are positive.

Differentiation of equation (1.2) with respect to ϵ yields an expression of the tangent modulus for the particular stress-strain relation which exists in the cross section at time, t.

One has in this case

$$\partial\sigma/\partial\epsilon = E_c - 2G(\epsilon - \epsilon_c) \tag{1.3}$$

Relation (1.3) shows that the tangent modulus decreases linearly as $\epsilon - \epsilon_c$ increases. Since the stress must increase monotonically with strain, it follows that the parabolic approximation is invalid for strain differences larger than the value given by the relation

$$E_c - 2G(\epsilon - \epsilon_c) = 0 \tag{1.4}$$

or

$$\epsilon - \epsilon_c = E_c/2G \tag{1.5}$$

We shall see later that the isochronous curves obtained from cross plotting creep-tension data under constant load are valid stress-strain relations for the lower bound to the solution. Figure 4 shows the degree to which relation (1.3) is satisfied for the isochronous curves of Stabilized 24S Aluminum

Alloy in the range of strains 0.5 to 1.5 x 10^{-3}. No particular importance should be attached to the fact that the lines are nearly parallel to each other.

Substitution of (1.1) in (1.2) gives

$$\sigma - \sigma_c = E_c y\eta'' - Gy^2 \eta''^2 \tag{1.6}$$

In accordance with Figure 3, compressive stresses and strains are counted as positive. A similar substitution in (1.5) gives

$$\eta'' y = E_c / 2G \tag{1.7}$$

The smallest tangent modulus occurs at the inner fiber, i.e., for $y = -h/2$. Hence, the largest absolute value of curvature is subjected to the condition

$$|\eta''|_{max} \leq E/Gh \tag{1.8}$$

With reference to Figure 1 the conditions of equilibrium of forces and moments read at any time, t as follows:

$$P = \int \sigma dA \tag{1.9}$$

and

$$P(\eta_t + \mu) = \int \sigma y dA \tag{1.10}$$

Upon substitution of (1.6) in (1.9) and (1.10) and integration we have

$$-P + \sigma_t A - G_t I \eta_t''^2 = 0 \tag{1.11}$$

and

$$P(\eta_t + \mu) + E_t I \eta_t'' = 0 \tag{1.12}$$

In these formulae μ is the initial deflection of the column under no load, η_t is the additional deflection under load at time, t. E_t is the

tangent modulus at the centroid at time, t. The modulus of curvature, G_t is a function of time only, but E_t is also a function of z by virtue of (1.5).

The Lower and Upper Bound Criteria

In order to derive suitable criteria for these bounds consider (see Figure 2) the stress-strain relation in a slightly curved column immediately after the application of load and examine the trend of this relationship with time. The points of interest are A_0 and B_0 referring to elements of the outer and inner fibers located at the midlength of the column. By symmetry, the deflection is maximum at this location. The time independent component of strain is assumed to follow Hooke's Law. Hence, the relevant points for all elements of the column at time zero are located on the straight line $A_0 B_0$. If no change of stress had occurred, the stress-strain relation after a time interval, t would be given by the isochronous curve $E_1 F_1$. However, the decreased stiffness of column causes larger deflections under applied load, and the ensuing increase of the bending moment calls for an increment in the stress difference. Consequently, the stress level of the inner fiber will be higher, as indicated by $A_0' A_1'$

The lower bound to the solution is obtained by locating the corresponding strain on the isochronous line, point A_1'. This can be shown as follows. The actual increase of strain is due to a gradual stress variation from level $A_0 E_1$ to level $A_0' A_1'$. It is, therefore, smaller than the strain $A_0' A_1'$ obtained by maintaining the stress at the higher level from the very beginning. That is, the actual point A_1 is to the left of A_1'. It can be shown likewise that the actual point B_1 referring to the outer fiber is to the right of B_1' located on the isochronous curve. If N

is the intersection between the actual and isochronous stress-strain diagrams, then by the assumed parabolic relationship the same increment of stress above N will cause a larger increment of the isochronous strain than of the actual strain. The isochronous stress-strain curve, therefore, corresponds to a less stiff column and gives larger deflections than the real one.

The upper bound is obtained by going to the other extreme. Instead of maintaining the outer fiber at the higher stress level $A_0' A_1'$ the fiber is supported at the lower stress level, $A_0 E_1$ and then allowed to reach the higher level $A_0' A_1'$ instantly (elastically) at the end of the time interval, t, by following the path $E_1 A_1''$ parallel to $A_0 B_0$. Since the time independent strain increment is only a part of the total strain increment, the corresponding point A_1'' will be to the left of A_1 . By a similar mode of reasoning point B_1'' will be to the right of B_1 . The repetition of the argument used in the case of the lower bound will then show that $B_1'' A_1''$ corresponds to a stiffer column than the real one and that it leads to smaller deflections.

To derive the necessary stress-strain relationship for the upper bound the stress and strain at the centroid are made to coincide with point C_1 of the isochronous curve. The parabola $B_1'' C_1 A_1''$ is then determined uniquely, as will be shown later, from the equilibrium of moments, hypothesis of plane sections, and prescribed paths $E_1 A_1''$ and $F_1 B_1''$ for the central elements of the extreme fibers. The constraints imposed thereby on the elements of the column are elastic by hypothesis. The solution, therefore, is an upper bound.

This solution can be greatly improved by adopting a step-by-step

procedure similar to that devised by Shanley (3). The first interval of time is made small enough to cause only a small difference of deflection between the stiffer and the real columns. Thereupon the stiffer column is made to deform (to creep) under constant stress again. As the column creeps the elastic constraints gradually disappear, and there comes a moment when the originally stiffer column acquires the same stiffness as the true column. The deflections of the two columns are then likewise the same. From that moment on the relation between the two columns becomes similar to that obtained at the beginning of the first time interval. It follows that by maintaining and relaxing the constraints in turn the whole argument can be repeated for the second, third, etc., time intervals.

This process is depicted schematically in the cut of Figure 2. The real column deflects according to the curve $A_1 A_2 A_3$; the deflection of the upper bound follows the trend $A_1 C_1 C_2$. $A_1 B_1$ and $C_1 B_2$ refer to periods of time when the column is supported during creep, $C_1 A_2$ corresponds to the lapse of time when the column creeps under additional (elastic) constraints.

While the exact moment of coincidence of the two deflected columns cannot be computed, the difference between their deflections can be kept small at all times by making the time intervals sufficiently short.

THE LOWER BOUND

It was pointed out previously that this bound is obtained by applying the parabolic (second order) approximation to isochronous curves. The solution reads in accordance with equation (1.12) if $\mu = a \sin \pi z/l$.

$$\eta_t + \mu = \frac{a \sin \pi z/l}{1 - P/P_t} \tag{2.1}$$

where

$$P_t = \pi^2 E_t I/l^2 \tag{2.2}$$

and E_t is the tangent modulus of the isochronous curve at the centroid at time t.

Using nondimensional quantities (see Notations), we can rewrite expression (2.1) to read, as follows, for the maximum deflection (at $z = l/2$):

$$w_t + e = \frac{e}{1 - p_t} \tag{2.3}$$

In general, the value of E_t figuring in (2.2) does not correspond to the stress level $\sigma_0 = P/A$. By assuming $\sigma_t = P/A$ the equation of equilibrium of forces is in error by an amount which, according to (1.11), Section 1, does not exceed the value

$$\sigma_t - \sigma_0 = \frac{G_t (\pi/l)^4 r^2 a^2}{(P_t/P - 1)^2} \tag{2.4}$$

The maximum relative error is thus

$$\frac{\sigma_t - \sigma_0}{\sigma_0} = \frac{4\pi^4 r^3}{l^4 h^2} \frac{G_t}{\sigma_0} \frac{e^2 p_t^2}{(1-p_t)^2} \tag{2.5}$$

But

$$p_t = \frac{P}{P_t} = \frac{\sigma_0 l^2}{\pi^2 E_t r^2} \tag{2.6}$$

Hence

$$\frac{\sigma_t - \sigma_0}{\sigma_0} = (2r/h)^2 \frac{G_t \sigma_0}{E_t^2} \left(\frac{e}{1 - p_t}\right)^2 \tag{2.7}$$

Formula (2.7) shows that as the ratio p_t approaches unity the error increases more and more rapidly. For a nearly perfect column, or e close to zero, the maximum error does not become significant until $1 - p_t$ assumes a value as small as e . However, at that time, the deflection also begins to assume increasingly large values. Consequently, for nearly perfect column the value of E_t in formula (2.2) can be taken at the level of the average stress, $\sigma_0 = P/A$ almost up to the time of collapse.

If the initial eccentricity, e is not close to zero, the error computed by formula (2.7) may become large enough to invalidate formula (2.1) as a lower bound. A recurrent correction is then applied to (2.1) at short intervals to keep the error small. This procedure, which is described in Section 4, results in values of w_t that are larger than those given by (2.3). That is, the critical time of collapse becomes shorter than for a nearly perfect column.

The results of computation for three initial eccentricities and two different stress levels with $l/r = 81.4$ are plotted in Figure 5. This computation was based on available creep tension data for Stabilized 24S Aluminum Alloy at 350°F (1). Figure 3 reproduces the isochronous curves derived from these data. The probable error attending their plotting has been estimated as ± 3%. At best, these curves have been drawn through four experimental points. For 120 hours only one point was available. The trend

of this isochronous curve is, therefore, highly hypothetical. Figure 4 shows the range of strains for which the parabolic approximation is valid with ± 8%.

The effect of increasing eccentricity, e on the time of collapse is clearly seen in Figure 5. The available experimental deflections for the two stress levels have been plotted as dashed lines in this Figure. It is seen that in actual tests the column exhibits a longer life not only when the effect of eccentricity is included in the computation, but also when it is disregarded. This finding suggests that for moderately crooked columns formula (2.1) could be used as a lower bound by taking the value of the tangent modulus E_t at the level of the average stress $\sigma_0 = P/A$, i.e., as if the column were perfectly straight. In the absence of a theoretical proof the justification for such a procedure can come only from the experiment.

The comparison between experimental and computed results can be enhanced by specifying a finite rather than infinite value of deflection as the criterion of failure. Accordingly, the time of collapse was chosen here arbitrarily as the time required by the column to reach a value of deflection at its midlength equal to the core radius, r_c or in nondimensional notation to have $w + e = 1$. It will be recalled that for a linear stress-strain relationship the value of $w + e = 1$ marks the beginning of stress reversal at the outer fiber. In the case of a parabolic stress-strain relationship the reversal occurs generally at values of $w + e$ lower than one. They approach, however, unity for sections having large core radii ratios, r_c/h, as e.g. in I beams and tubular columns. (See Appendix A.)

In Figure 6 the loads, or stresses, expressed as P/P_0 have been

plotted against the log of time necessary to produce the specified deflection, $w + e = 1$ at the midlength of column. The time computed for a given load was adjusted by interpolation to correspond to about the same eccentricity as that indicated for the experimental curves. It is seen that the discrepancy between the lower bound and actual data is much smaller if the comparison is based on stresses for a given collapse time rather than collapse times for a given stress. This is to be expected in view of the logarithmic trend indicated by the nearly straight line of the semi-log plot.

THE UPPER BOUND

The recurrent procedure for the determination of the upper bound has been outlined briefly in a previous section. This procedure will now be described in detail.

Let $A_{t-1}\ C_{t-1}\ B_{t-1}$ (see Figure 7) represent the stress-strain relationship for the upper bound at time $t-1$. The points A_{t-1} and B_{t-1} refer to elements of the two extreme fibers at the midlength of column, while point C_{t-1} refers to the centroid of the cross-section. The problem consists of obtaining the stress-strain relationship (and the deflection) at time t.

To this end the column is deformed in the interval of time following $t-1$ in such a way that the stress remains constant in each element. On the assumption that strain rates are path independent, the strain increments for this interval can be read at the same stress level from the corresponding isochronous curves, $GC_{t-1}\ D$ and $HC_t\ F$.* Thus points K and E are obtained by making $B_{t-1}K = GH$ and $A_{t-1}E = DF$. Next, the constraints are relaxed instantly at K and E, whereby these points are made to follow the paths EA_t and KB_t parallel to OC_0, which is the stress-strain relation at time zero. The points A_t and B_t are located by drawing a parabola $B_tC_tA_t$ in such a way that all conditions imposed on the column are satisfied except the condition of equilibrium of forces.

*For convenience these curves have been drawn through the points C_{t-1} and C_t corresponding to the centroid. The location of C_{t-1} is explained in the next section.

The error introduced by this approximation is minimized subsequently by the procedure described in the next section.

The remaining conditions are obtained as follows. The assumption of parabolic stress-strain law gives (see Figure 7),

$$\sigma_A - \sigma_{t-1} = E_t \Delta_t \epsilon/2 - G_t \left(\frac{\Delta_t \epsilon}{2}\right)^2 \tag{3.1}$$

and

$$\sigma_B - \sigma_{t-1} = - E_t \Delta_t \epsilon/2 - G_t \left(\frac{\Delta_t \epsilon}{2}\right)^2 \tag{3.2}$$

hence by subtracting (3.2) from (3.1) and putting $\Delta_t \sigma$ for $\sigma_A - \sigma_B$

$$\Delta_t \sigma = E_t \Delta_t \epsilon \tag{3.3}$$

In variance with the lower bound, E_t is not known, but it can be determined if three more relations are added to (3.3). These are:

1) the equilibrium moments, viz.

$$P(\eta_t + \mu) + E_t I \eta_t'' = 0 \tag{3.4}$$

2) the hypothesis of plane section, viz.

$$\Delta_t \epsilon = \eta_t'' h \tag{3.5}$$

and, 3) a recurrent formula which is easily derived from Figure 7 and which reads

$$\Delta_t \sigma = \Delta_{t-1} \sigma + E_0 (\Delta_t \epsilon - \Delta_t' \epsilon) \tag{3.6}$$

In this formula, E_0 is the slope of OC_0. We thus have four equations (3.3), (3.4), (3.5), and (3.6) from which the four unknowns, $\Delta_t \sigma$, $\Delta_t \epsilon$, E_t, and η_t can be determined.

If the initial deflection μ is in the form of a sinusoid the manipulation of the above four equations yields the following expression for the maximum deflection:

$$a_t = \frac{Pa + E_0 \Delta'_t \epsilon I/h - \Delta_{t-1} \sigma I/h}{\pi^2 E_0 I/l^2 - P} \tag{3.7}$$

hence

$$a_t + a = \frac{\pi^2 E_0 Ia/l^2 + E_0 \Delta'_t \epsilon I/h - \Delta_{t-1} \sigma I/h}{\pi^2 E_0 I/l^2 - P} \tag{3.8}$$

or using nondimensional quantities

$$w_t + e = \frac{2\sigma_{cr} e + E_0 \Delta'_t \epsilon - \Delta_{t-1} \sigma}{2(\sigma_{cr} - \sigma_0)} \tag{3.9}$$

This can be written also as

$$w_t = w_0 + \frac{E_0 \Delta'_t \epsilon / 2\sigma_{cr} - \Delta_{t-1} \sigma / 2\sigma_{cr}}{1 - \nu_0} \tag{3.10}$$

It is easy to see that the second term on the r.h.s. of (3.9) is positive and that it increases rapidly as $\Delta'_t \epsilon$ becomes larger and larger. In particular for $w_t + e = 1$ formula (3.9) gives

$$E_0 \Delta'_t - \Delta_{t-1} \sigma = 2[\sigma_{cr}(1 - e) - \sigma_0] \tag{3.11}$$

In order to start the recurrent procedure $\Delta_{t-1} \sigma$ is computed for time $t = 0$ by assuming an elastic behavior. The deflection after the first time interval is then obtained from formula (3.7). Next $\Delta_t \epsilon = \Delta_1 \epsilon$ is computed by means of formula (3.5) and the points A_1 and B_1 similar to A_t and B_t, are located on the stress-strain diagram using the construction shown in Figure 7. This gives $\Delta_{t-1} \sigma = \Delta_1 \sigma$, the starting point for the next time interval, etc. An example of the recurrent procedure is shown in Figure 8.

It will be noticed that the knowledge of σ_t and G_t is not required for

the computation of deflection. This is so because the condition of equilibrium of forces was not considered.

In the course of this investigation it was found that the quantity by which the equilibrium of forces was in error was considerably smaller for the upper bound than for the lower one. In many cases, especially in the beginning, the correction described in the next section could be entirely disregarded. This circumstance reduces substantially the labor of computation.

The results of computation for 3 initial eccentricities and 2 stress levels with $l/r = 81.4$ are plotted in Figure 9. The same basic data were used for this plot as in the case of the lower bound.* The available experimental data are plotted as dashed lines. It is seen that the experimental deflections are initially smaller than the corresponding upper bound. This contradiction must be ascribed to the approximation attending the experimental determination of the initial eccentricity, e . We have found that if the initial deflection is chosen, by cut and trial, so that formula (3.7) reproduces the measured deflection after $2\frac{1}{2}$ hours, the recurrent procedure carried from that moment on provides a closer match and the correct relationship between experiment and computation, as evidenced by Figure 10. This circumstance would seem to call for duplicate tests aimed at the establishment of the scatter experimental data before any definite conclusions can be drawn.

---

* The part of the curves drawn by means of dotted lines represents a probable trend inferred from the fact that the highest stress level at the inner fiber for 60 hours no longer intercepts the 120 hours isochronous curve within the range of available data.

On comparing values of P/P_0 corresponding to the same eccentricity and the same "collapse" time, it is found (see Figure 6) that the discrepancies between computation and experiment are much smaller for the upper bound than for the lower one. Should this result be confirmed by further investigations a more refined procedure for the upper bound would be in order to obtain an even closer agreement with the experiment.

CORRECTION FOR THE STRESS AT THE CENTROID

The procedures which have been described previously for both the upper and lower bounds were shown to introduce an error in the equation of equilibrium of forces, an error which increases with time. An approximate method developed in this section permits a recurrent correction of this error at small time intervals.

We start with the first time interval. Because of the nonlinear nature of the stress-strain relationship the stress at the centroid departs during this interval from the initial value, $\sigma_0 = P/A$ (see Figure 11), the more the closer the cross section to the midlength of the column. At time t_1 the stress at the centroid will assume values ranging from σ_0 at point D_1 to a maximum value at some point H_1. If $\Delta\sigma$ is the increase of stress (over σ_0) at a given level, z of the column then by (1.11), Section 1

$$\Delta\sigma = G_1 r^2 \eta_1''^2 \tag{4.1}$$

The time interval can always be chosen small enough to approximate D_1H_1 by the tangent at D_1. Thus

$$\Delta\sigma = E_1 \Delta\epsilon \tag{4.2}$$

where E_1 is the tangent modulus at D_1.

On the other hand, see (1.3), Section 1

$$\Delta E = -2G\Delta\epsilon \tag{4.3}$$

hence,

$$\frac{\Delta E}{E_1} = -\frac{2G_1}{E_1^2}\Delta\sigma = -\frac{2G_1\sigma_0}{E_1^2}\frac{\Delta\sigma}{\sigma_0} \tag{4.4}$$

That is, to the order of approximation considered, $\Delta E/E_1$, is proportional to and of the same order of magnitude as $\Delta\sigma/\sigma_0$.*

If η in (4.1) can be approximated by a sinusoid then $\Delta\sigma$ will vary as $\sin^2 \pi z/l$ and so will ΔE by (4.4). On this assumption we can write

$$E = E_1 + \Delta E_1 \sin^2 \pi z/l \tag{4.5}$$

where ΔE_1 is the maximum change of E_1.

Substitution of (4.5) in the equation of equilibrium of moments yields, see (1.12), Section 1

$$P(\eta + \mu) + (E_1 + \Delta E_1 \sin^2 \pi z/l) I \eta'' = 0 \tag{4.6}$$

or

$$\eta'' + \frac{P}{E_1 I (1 + \frac{\Delta E_1}{E_1} \sin^2 \pi z/l)} (\eta + \mu) = 0 \tag{4.7}$$

By (1.3) ΔE_1 is negative. Hence the actual deflection will be larger than for E_1 but it will be smaller than for $E_1 + \Delta E_1$. In other words, there exists a fraction k such that the actual deflection will be given by the equation

$$\eta'' + \frac{P}{E_1 I (1 + k\, \Delta E_1/E_1)} (\eta + \mu) = 0 \tag{4.8}$$

provided the sinusoidal approximation is valid. The validity of this approximation for small values of $\Delta E_1/E_1$ is justified in Appendix B. It is also shown there that for a sine square variation of $\Delta\sigma$, $k = \frac{1}{4}$. Substitution of $k = \frac{1}{4}$ in (4.8) yields the solution for η as follows

$$\eta_1 = \frac{\mu}{P_1/P - 1 + \Delta P_1/P} \tag{4.9}$$

---

* G is of the order of 10^9, σ_0 of the order of 10^5, and E_1^2 of the order of 10^{12}.

where

$$\mu = a \sin \pi z/l \tag{4.10}$$

$$P_1/P = (\pi r/l)^2 E_1/\sigma_0 \tag{4.11}$$

and

$$\Delta P_1/P = -\tfrac{1}{4}(\pi r/l)^2 \frac{2G_1}{E_1}\frac{\Delta\sigma_1}{\sigma_0} = \tfrac{1}{4}\left(\frac{\pi r}{l}\right)^2 \frac{\Delta E}{\sigma_0} \tag{4.12}$$

Differentiating (4.9) twice and substituting the result in (4.12) one has the relation

$$\Delta\sigma_1 = \frac{(\pi/l)^4 a^2 r^2 G_1}{\left[P_1/P - 1 - \frac{3}{4}(\pi r/l)^2 \frac{2G_1}{E_1}\frac{\Delta\sigma_1}{\sigma_0}\right]^2} \tag{4.13}$$

from which $\Delta\sigma_1$ can be determined and point H_1 located in Figure 11. Inspection of formula (4.12) shows that the deflection is computed as though the stress at the centroid were at the level C_1 for all sections of the column and its value were

$$\sigma_1 = \sigma_0 + \tfrac{1}{4}\Delta\sigma_1 \tag{4.14}$$

Hence, formula (4.14) can be considered as the required correction for the centroid.

In order to derive the general formula consider the second time interval. It is easy to see from (2.4), Section 2 and the formulae (4.13) and (4.14) that the correction for the second time interval reads (see Figure 11),

$$\sigma_2 = \sigma_1 + \tfrac{1}{4}\Delta\sigma_2 \tag{4.15}$$

and

$$\Delta\sigma_2 + \sigma_1 - \sigma_0 = \frac{(\pi/l)^4 a^2 r^2 G_2}{\left[P_2/P_1 - 1 - \tfrac{1}{4}(\pi r/l)^2 \frac{2G_2}{E_2}\frac{\Delta\sigma_2}{\sigma_0}\right]^2} \tag{4.16}$$

Thus $\Delta\sigma_2$ can be determined from (4.16).

If the above relations are generalized there follows that

$$\eta_t = \frac{\mu}{P_t/P - 1 + \Delta P_t/P} \tag{4.17}$$

where

$$\frac{P_t}{P} + \frac{\Delta P}{P} = \left(\frac{\pi r}{l}\right)^2 \left[\frac{E_t}{\sigma_0} - \frac{3}{2}\frac{G_t}{E_t}\frac{\Delta\sigma_t}{\sigma_0}\right] \tag{4.18}$$

and E_t is the tangent modulus for the time t, at the level of stress $\Delta\sigma_t$ Similarly

$$\Delta\sigma_t + \sigma_{t-1} - \sigma_0 = \frac{G_t (\pi/l)^4 a^2 r^2}{\left[\frac{P_t}{P} - 1 - \frac{3}{2}\left(\frac{\pi r}{l}\right)^2 \frac{G_t}{E_t}\frac{\Delta\sigma_t}{\sigma_0}\right]^2} \tag{4.19}$$

from which $\Delta\sigma_t$ can be determined.

It is to be noted that formulae (4.17), (4.18), and (4.19) have been derived under the assumption of small stress increments, $\Delta\sigma_t$. By virtue of (4.1) large increments of σ_t also imply large increments of deflection. Hence, the limit of validity of the above assumption coincides with the beginning of large deflection rates, i.e., very nearly with the collapse of the column.

In the course of this investigation a somewhat less rigorous but more rapid procedure has been adopted. This procedure is particularly suited to the upper bound. To explain its application assume (see Figure 12), that the column is supported during the first interval of time so that each element deflects with the same stress σ_0 at the centroid. The deflection is then computed with the tangent modulus, E_1^* at the level σ_0 instead of the tangent modulus E at the level $\sigma_1 = \sigma_0 + \frac{1}{2}\Delta\sigma_1$ as in the previous

procedure. Hence

$$\eta_1^* = \frac{\mu}{P_1^*/P - 1} \tag{4.20}$$

where

$$P_1^*/P = \left(\frac{\pi r}{l}\right)^2 \frac{E_1^*}{\sigma_0} \tag{4.21}$$

and the asterisk is used to avoid confusion of formulae. Next, the constraints on the centroids are relaxed, whereupon the stress at the centroid increases elastically at each level z by the amount given previously, i.e., by

$$\Delta\sigma = G_1 r^2 \eta''^2 \tag{4.22}$$

The maximum increment is at the level $z = l/2$ and has the value as follows at the beginning of the second interval:

$$\Delta\sigma_1^* = \frac{(\pi/l)^4 r^2 a^2 G_1}{(P_1^*/P - 1)^2} \tag{4.23}$$

The column is now supported during the second time interval so that each element dz of the column deflects with the stress increments at the centroid imposed by (4.22). Proceeding as previously we obtain at the end of the second interval the deflection

$$\eta_2^* = \frac{\mu}{P_2^*/P - 1} \tag{4.24}$$

where

$$\frac{P_2^*}{P} = \left(\frac{\pi r}{l}\right)^2 \left[\frac{E_2^*}{\sigma_0} - \frac{3}{2}\frac{G_2}{E_2^*}\frac{\Delta\sigma_1^*}{\sigma_0}\right] \tag{4.25}$$

and E_2^* is the tangent modulus at the level of σ_0, point D_2^* (see Figure 12). Accordingly, the increment of stress at the midlength of column is as follows at the beginning of the third time interval:

$$\Delta\sigma_2 = \frac{(\pi/l)^4 G_2 a^2 r^2}{(P_2^*/P - 1)^2} \tag{4.26}$$

More generally one can write that

$$\eta_t^* = \frac{\mu}{(P_t^*/P - 1)} \tag{4.27}$$

where

$$P_t^*/P = \left(\frac{\pi r}{l}\right)^2 \left[\frac{E_t^*}{\sigma_0} - \frac{3}{2}\frac{G_t}{E_t^*}\frac{\Delta\sigma_{t-1}^*}{\sigma_0}\right] \tag{4.28}$$

and E_t^* is the tangent modulus for time t but at the stress level σ_{t-1}^*

Likewise,

$$\sigma_t^* = \sigma_{t-1}^* + \frac{3}{4}\Delta\sigma_{t-1}^* \tag{4.29}$$

where

$$\Delta\sigma_{t-1}^* + \sigma_{t-2}^* - \sigma_0 = \frac{(\pi/l)^4 a^2 r^2 G_{t-1}}{(P_{t-1}^*/P - 1)^2} \tag{4.30}$$

Since the corrections to the centroidal stress are made a posteriori, obviously, if (4.17) and (4.27) are compared

$$\eta_t^* < \eta_t$$

However, E_t^* is generally smaller than E_{t-1}, and G_t is larger than G_{t-1}, hence on the assumption of nearly equal stress increments $\Delta\sigma_{t-1}$ and $\Delta^*\sigma_{t-1}$ we can write that $\eta_t > \eta_t^* > \eta_{t-1}$.

In other words, the error involved in the simplified procedure is of the order of

$$\eta_t - \eta_{t-1}$$

and it is small, if the time intervals are small.

THE SEMI-ELASTIC COLUMN

The procedures described previously were restricted to columns subjected to a relatively high average stress. For such columns the relevant portion of the isochronous curve could be approximated by a parabola for all fibers of the column. As the slenderness ratio increases the average stress must be lowered. A value may finally be reached such that the stress-strain relationship becomes linear and time independent in the outer fibers, while remaining nonlinear and time dependent in the inner fibers. This situation is depicted schematically in Figure 13. B_0, B_1, B_2 represent the relation between stress and strain at the outer fiber, while A_0, A_1, A_2 refer to the same relationship at the inner fibers for times $t = 0$, t_1, $t_2 \cdots$ There is an apparent similarity between this case and that treated by van Karman (11). If the isochronous curves represented the correct stress-strain relationship, the procedure devised by van Karman would give the exact solution. Moreover, modern computational methods would allow this solution to be obtained with relative ease. However, the isochronous curves can be used only as a lower bound for the solution. Under these circumstances it appeared more profitable to seek a somewhat less rigorous, but more rapid method of solution. A glance at Figure 13 shows that the tangent modulus at the average stress level cannot be used in the computation of a lower bound. To do so would be to assume a constant deflection which is independent of initial eccentricity. This assumption is contradicted by experiment. Not only does the deflection vary with time but it may become rapidly large enough to cause instability of the column. Consideration of initial eccentricity appears to be paramount

in this case, a fact pointed out previously by Rosenthal and Baer (8). Figure 13 refers to the limiting case when all fibers having stresses lower than the average follow the linear, time independent, trend, while all fibers having stresses larger than the average follow a parabolic, time dependent, trend.* The method of solution involves essentially the same steps as in the case of a fully parabolic stress-strain relationship. First, the deflections are computed from the condition of equilibrium of moments by maintaining the stress constant at the centroid. Next, a correction is applied to the centroidal stress to reduce the error in the condition of equilibrium of forces.

Deflection for a Constant Stress at the Centroid

With reference to Figure 13, the fundamental equations of Section 1 read as follows**

$$\sigma = \sigma_0 + E_0 \eta'' y \qquad \text{for} \quad h/2 > y > 0 \tag{5.1}$$

and

$$\sigma = \sigma_0 + E_t \eta'' y + G_t \eta''^2 y^2 \qquad \text{for} \quad -h/2 < y < 0 \tag{5.2}$$

The condition of equilibrium of moments becomes, as easily seen

$$P(\eta + \mu) + \frac{E_0 + E_t}{2} I\eta'' + G_t J\eta''^2 = 0 \tag{5.3}$$

where

$$J = \int_0^{h/2} y^3 dA \tag{5.4}$$

Failing to reduce equation (5.3) to listed types of nonlinear equations (12) we have endeavored to obtain solution of this equation by means of

---

* The manner in which this treatment can be extended to other cases must be reserved to future studies.

** The use of a parabolic approximation requires here two different tangent moduli, E_0 and E_t at point C.

differential analyzer. Concurrently two procedures of approximate solutions have been worked out. They are described in Appendices E and F.

For the purpose of computation equation (5.3) was put in a nondimensional form by making substitutions as follows:

$$\zeta = \pi z/l \tag{5.5}$$

$$\phi = \eta/a \tag{5.6}$$

$$\omega = 2Pl^2/\pi^2(E_0 + E_t)I \tag{5.7}$$

$$\alpha = 2G_t J a\pi^2/(E_0 + E_t)Il^2 \tag{5.8}$$

Equation (5.3) then becomes

$$\phi'' + \omega(\sin\zeta + \phi) + \alpha\phi''^2 = 0 \tag{5.9}$$

with

$$\phi = \phi'' = 0 \qquad \text{for} \qquad \zeta = 0 \quad \text{and} \quad \pi \tag{5.10}$$

Typical deflection curves traced by the differential analyzer are reproduced in Figure 14. Despite the presence of the squared term in equation (5.9) the general shape of a sinusoid is preserved in the solution. Slight deviations from the sine function occur only near the ends for $\zeta = 0$ and π where the curve is slightly flatter. Figure 15 cumulates the values of maximum deflection, f (at $\zeta = \pi/2$) for various combinations of ω and α. It is seen that there are values of ω and α for which no solution exists. These values cover a domain for which the assumed approximations violate the condition of equilibrium of moments. Either a different stress-strain relation or a different lower bound must then be assumed.

It has been pointed out in Section 1 that the parabolic approximation is subject to the condition that the stress must be everywhere a monotonic function of strain. This condition reads as follows (see (1.8), Section 1),

$$|\eta''|_{max} < \frac{E_t}{G_t h} \tag{5.11}$$

Using relations (5.5) to (5.8) we have

$$|f''| < \frac{kJ}{\alpha I h} \tag{5.12}$$

where

$$k = 2E_t/(E_t + E_0) \tag{5.13}$$

Inspection of an actual case (see Appendix C) shows that for small deflections condition (5.12) imposes more stringent restrictions on ω and α than the condition of equilibrium of moments.

The case of larger deflections was not considered. However, at larger deflections the change of stress at the centroid would make the value of E_t in (5.13) and consequently, the value of k in (5.12) smaller. It can be shown (see Appendix C) that in the case considered a 10% decrease in k is sufficient to make condition (5.12) the more restrictive one even for large deflections.

It is concluded that when G and E are adjusted in the parabolic approximation so as to comply with condition (5.11) the obtained stress-strain relationship can in general also be used for the establishment of a lower bound for a partly elastic column.

Correction for the Stress at the Centroid

The exact correction for the centroidal stress can be obtained only by solving simultaneously equations of equilibrium of forces as well as moments,

i.e., by following essentially the method of van Karman (11).

The less rigorous procedure adopted here involves two approximations:

1. The corrections are made a posteriori, i.e., after the deflections have been determined. It was pointed out at the end of Section 4 that this procedure amounts to making the column somewhat stiffer, the less so, however, the more frequently the corrections are made.
2. After the stress at the centroid has been corrected the part of the isochronous curve below the centroid, point C_2, Figure 16, is replaced by a straight line through the origin O, such as OC_2. Since the corrections of the centroidal stress vary from zero at the ends of the column to a maximum at its midlength, the slopes of the straight lines through the origin will also be variable. We shall further assume that these slopes vary with the distance z in the same manner as the correction of the stress at the centroid. This assumption is based on the validity of small deformations.

Like the first approximation, the replacement of the broken line, OC_0C_2 by the straight line OC_2 makes the column somewhat stiffer. However, the analysis of an actual case (see Appendix D) shows that the increase of stiffness is less than 3% if the total increase of stress at the centroid is less than 20%.

With these two approximations the correction of the centroidal stress follows essentially the recurrent procedure of Section 4.

It will suffice to retrace here the first two steps only.

The column (see Figure 16), is supported during the first time interval in such a way that each element of the column deflects with the same stress σ_0 at the centroid. The deflection is then determined at time t_1 by putting $E_t = E_1$ and $G_t = G_1$ in formulae (5.3) to (5.9). It was previously pointed out that the solution of (5.9) is very close to a sinusoid. Hence, if f_1 is obtained from the plot (Figure 15), one can write

$$\phi_1 = f_1 \sin \zeta \tag{5.14}$$

or reverting to linear dimensions

$$\eta_1 = \frac{a \sin \pi z/l}{P_1/P - 1} = a_1 \sin \pi z/l \tag{5.15}$$

Here by definition and for convenience we put

$$P_1/P - 1 = 1/f_1 \tag{5.16}$$

P_1 can be called the substitute Eulerian load which gives the same solution as equation (5.3) to a very close approximation. Next, the constraints on the centroids are relaxed, whereupon the stress at the centroid increases elastically at each level z by an amount such that the condition of equilibrium of forces is satisfied. Integration of equations (5.1) and (5.2) yields for this condition the relation

$$P = \sigma A + (E_0 - E_1) S \eta_1'' - G_1 I \eta_1''^2/2 \tag{5.17}$$

where S is the static moment of half the cross sectional area. Hence, by (5.15) the increase of stress, $\Delta\sigma$ at the centroid

$$\Delta\sigma = (E_0 - E_1) \frac{\pi^2 s a_1}{l^2} \sin \frac{\pi z}{l} + \frac{G_1}{2} (\pi/l)^4 a_1^2 r^2 \sin^2 \pi z/l \tag{5.18}$$

where

$$s = S/A \tag{5.19}$$

The maximum increment is at the level $z = l/2$ and it has the following value at the beginning of the second interval, point H_1 (Figure 16),

$$\Delta\sigma_{max} = \frac{G_1}{2}(\pi/l)^4 r^2 a_1^2 (1 + \gamma_1) \tag{5.20}$$

where

$$\gamma_1 = \frac{2(E_0 - E_1)l^2 s}{G_1 \pi^2 r^2 a_1} \tag{5.21}$$

The column is now supported during the second interval so that each element dz deflects with the stress increments at the centroid imposed by (5.18). The time interval can be chosen small enough to approximate $C_0 H_1$ by the tangent at C_0. Thus

$$\Delta\sigma = E_1 \Delta\epsilon \tag{5.22}$$

On the other hand

$$\Delta E = -2G_1 \Delta\epsilon \tag{5.23}$$

hence

$$\Delta E_1 = -2G_1 \Delta\sigma_1 / E_1 \tag{5.24}$$

By an argument similar to that used in Section 4, it follows that one can write a correction for E_2 in the form

$$\Delta E = \Delta E_2 (\sin^2 \pi z/l + \gamma_1 \sin \pi z/l) \tag{5.25}$$

where ΔE_2 is the maximum change of E_2. Substitution of (5.25) in the equation of equilibrium of moments yields for time t_2.

$$P(\eta + \mu) + \left[\frac{E_0 + E_2}{2} + \Delta E_2 (\sin^2 \pi z/l + \gamma_1 \sin \pi z/l)\right]\eta'' + G_2 J \eta''' = 0 \tag{5.26}$$

It was previously pointed out that for $\Delta E_2 = 0$ the deflection can be put in the form of a sinusoid; hence, the procedures described in Appendices B and E are applicable, and the solution of (5.26) can be obtained

by superposition of corrections for $\sin^2 \pi z/l$ and $\sin \pi z/l$. The correction for the stress at the centroid thus reads

$$\Delta\sigma_1 = \frac{G_1}{2} (\pi/l)^4 r^2 a_1^2 (0.75 + 0.85 \gamma_1) \tag{5.27}$$

By analogy with (4.24), Section 4

$$\eta_2 = \frac{\mu}{P_2^*/P - 1} \tag{5.28}$$

However, P_2^*/P has here a somewhat different form. If we put by analogy with (5.16)

$$P_2/P - 1 = 1/f_2 \tag{5.29}$$

then

$$P_2^*/P - 1 = P_2/P - 1 + \Delta P_2/P \tag{5.30}$$

and

$$\Delta P_2/P = - \left(\frac{\pi r}{l}\right)^2 \frac{2G_2}{E_2} \frac{\Delta\sigma_1}{\sigma_0} \tag{5.31}$$

Since the tangent modulus, E in this case is measured only at one stress level the star over E_2 has been omitted.

Inspection of formula (5.31) shows that the deflection η_2 is computed as though the stress at the centroid were at the level $\sigma_1 + \Delta\sigma_1$ for all sections of the column, point C_2 (Figure 16). Hence, formula (5.27) can be considered as the required correction for the centroid.

From the above discussion the rules for computing the deflection at time t_2 can be stated as follows:

1. Find the location of C_2 by means of formula (5.27).
2. Join C_2 to the origin 0.
3. Determine the deflection η_2 from the slope of the line OC_2,

say E_s^0, (instead of E_0), and the tangent C_2N_2 at point C_2 using formulae (5.7) and (5.8) and the set of curves of Figure 15.

Once the deflection η_2 has been determined the correction to the stress at the centroid is available by using a formula analogous to (5.27). The procedure can therefore be carried to the next interval of time, etc.

Results

Figure 17 shows the deflections computed by the above procedure for Stabilized 24S Aluminum Alloy at the level $P/P_0 = 0.72$, $l/r = 131$, using the isochronous curves (Figure 3) for 350°F. and three different initial eccentricities as indicated. The curve drawn by means of dashed lines represents the available experimental data at this stress level. It is seen that the experimentally determined time for attaining a given value of deflection is longer for the same initial eccentricity. It would seem, therefore, that the computed deflections are still a lower bound despite the two "stiffening" approximations made. This conclusion cannot be accepted unreservedly since the scatter of experimental data is not known.

If the computed "collapse" time, for attaining a deflection $w + e = 1$ is plotted on the experimentally determined stress-collapse time curve at the same l/r and e, the computed point falls very near to the curve (see Figure 6). An attempt to work out an upper limit to the solution using the procedure of Section 3 led to unacceptably small deflections. It would therefore appear that for the semi-linear stress-strain relation, the lower bound is much closer to the solution than for the parabolic one.

CONCLUSIONS

The purpose of this investigation was to compute time-deflection curves of columns under compressive loads using creep tension data. The computation is based on the usual assumptions of the beam theory and an additional assumption regarding the stress variation in the cross section. It is assumed that this variation can be approximated by a parabola in terms of the position in the plane of bending. The investigation leads to conclusions as follows:

1. An upper and a lower bound can be assigned to the deflection at any time, using isochronous curves derived from creep tension data.
2. The lower bound is obtained by putting the value of the tangent modulus to the isochronous curve at time, t in the Euler formula for initially curved columns. The tangent modulus is read at stress levels which are higher than the average stress, the higher above the average, the greater the initial eccentricity and the longer the time.
3. For perfectly straight columns the tangent modulus remains at the average stress level up to the time corresponding to the "critical" value of the tangent modulus in the Euler formula. This time may be conveniently designated as the "collapse" time of a perfectly straight column.
4. The upper bound is obtained from the isochronous curves by a procedure of recurrent relaxation and imposition of constraint on the column. The procedure is applicable to prismatic columns of any type.

5. Comparison with experimental data on Stabilized 24S Aluminum Alloy at 350°F. suggests that the upper bound is a closer approximation to the solution than the lower one. There is further indication that for moderately crooked columns the tangent modulus at the average stress level supplies a sufficiently safe lower limit. The solution for this case can then be determined directly from the corresponding isochronous curve. In the absence of a theoretical proof the justification for the above procedure must come directly from the experiment.

6. The extension of computation to columns with high slenderness ratio results in considerable mathematical difficulties owing to the fact that only part of the column undergoes creep. The solution appears to depend critically on the initial eccentricity, a result which is in qualitative agreement with the experiment.

RECOMMENDATION FOR FUTURE WORK

Experimental

On the basis of the results obtained, future experiments are recommended as follows:

1. Creep tension data at low stress levels to determine more accurately the trend of isochronous curves for industrially important alloys.
2. Creep buckling tests on a series of identically loaded specimens to determine the statistical scatter of experimental results.
3. Creep buckling tests on models of columns with high slenderness ratio to check more carefully their sensitivity to initial deflections, as indicated by the theory.

Theoretical

1. Extension of computation to industrial alloys for which creep buckling data are already available, e.g., 24S-T6 Aluminum Alloy.
2. Refinement of the upper bound solution in an attempt to find an agreement with experiment that is close enough for safe design.
3. Improvement of the solution for high slenderness ratios.

BIBLIOGRAPHY

1. Carlson, R. L. and Schwope, A. D. Battelle Technical Report. WADC 52-251, Part I, (September 1952).

2. Hazlet, T. H., Parker, E. R. and Hansen, R. D. Journal of Metals. February 1953, p. 318.

3. Shanley, F. R. Weight Strength Analysis of Aircraft Structures. McGraw-Hill, 1952, p. 343.

4. Higgins, Jr., T. P. p. 359 of book cited in Reference 3.

5. Libove, C. Journal of Aeronautical Sciences, No. 19, p. 459, (July 1952).

6. Hoff, N. J. Journal of the Royal Aeronautical Society. No. 58, p. 1, (January 1954).

7. Kempner, J. N.A.C.A., TN 3136, TN 3137, (January 1954).

8. Rosenthal, D. and Baer, H. W. Proceedings of the First U. S. National Congress of Applied Mechanics, ASME, p. 603. 1952.

9. Orowan, E. same publication as Reference 8, p. 453.

10. Sherby, O. D., Orr, R. L. and Dorn, J. E. Journal of Metals. January 1954, p. 71.

11. van Karman, Th. Investigation of Buckling Strength. Forschungsarbeiten, V.D.I., No. 81. Berlin. 1910.

12. Kamke, Erich. Differentialgleichungen, Volume 1. Leipzig. 1943.

APPENDIX A.

Stress Reversal at Outer Fiber

The condition of stress reversal at the outer fiber is obtained by putting $y = \frac{h}{2}$ in equation (1.6), Section 1 and writing

$$\sigma = \sigma_t + E_t \eta'' \frac{h}{2} - G_t \eta''^2 \frac{h^2}{4} = 0 \tag{A.1}$$

On the other hand, the conditions of equilibrium of forces and moments read

$$\sigma_t = \sigma_0 + G_t \eta''^2 r^2 \tag{A.2}$$

and

$$\sigma_0 (\eta + \mu) = - E_t \eta'' r^2 \tag{A.3}$$

Substitution of (A.3) and (A.2) in (A.1) yields after division by a common factor

$$1 - \frac{(\eta + \mu)h}{2r^2} - \frac{G_t \sigma_0}{E_t^2} \frac{(\eta + \mu)^2 h^2}{4r^4} \left[1 - \frac{4r^2}{h^2}\right] = 0 \tag{A.4}$$

or in nondimensional notations

$$1 - (w + e) = \frac{G_t \sigma_0}{E_t^2} (w + e)^2 \left[1 - \frac{4r^2}{h^2}\right] \tag{A.5}$$

Inspection of (A.5) shows that in general $w + e < 1$. However, for high core radii ratios, r_c/h, $r \to h/2$, hence, $w + e \to 1$.

APPENDIX B

Solution of Equation (4.7), Section 4 by Perturbation Method

Since $\Delta E/E$ is small the above equation can also be written as follows:

$$\eta'' + \frac{P}{EI}\left(1 - \frac{\Delta E}{E}\sin^2 \pi z/l\right)(\eta + \mu) = 0 \tag{B.1}$$

Equation (B.1) is of the type of Mathieu's equations. The solution of this equation in terms of periodic Mathieu functions has been indicated.* For our present purpose it is more convenient to solve (B.1) approximately by means of sine functions using the perturbation method.** To this end rewrite (B.1) as follows:

$$\eta'' + \frac{P}{EI}\left[\left(1 - k\frac{\Delta E}{E}\right) + \frac{\Delta E}{E}\left(k - \sin^2 \pi z/l\right)\right](\eta + \mu) = 0 \tag{B.2}$$

where k is a constant to be determined. For convenience put

$$\frac{P}{EI}\left(1 - k\frac{\Delta E}{E}\right) = \frac{P'}{EI} = \omega^2 \text{ ***} \tag{B.3}$$

and

$$\frac{P}{EI}\frac{\Delta E}{E} = \beta \tag{B.4}$$

Also represent the operation of differentiation of second order by D^2 . There follows:

$$D^2\eta + \omega^2(\eta + \mu) + \beta(k - \sin^2 \pi z/l)(\eta + \mu) = 0 \tag{B.5}$$

---

* Theory and Applications of Mathieu Functions, by N. W. McLachlan, Oxford, 1951.

** Ordinary Nonlinear Differential Equations, N. W. McLachlan, Oxford, 1950.

*** Not to be confused with ω defined in Notations.

Assume a solution of the form

$$\eta = \eta_0 + \beta\eta_1 \tag{B.6}$$

such that

$$D^2\eta_0 + \omega^2(\eta_0 + \mu) = 0 \tag{B.7}$$

Since

$$\mu = a\sin \pi z/l \tag{B.8}$$

the solution of (B.7) reads

$$\eta_0 + \mu = a_0 \sin \pi z/l \tag{B.9}$$

where

$$a_0 = \frac{a}{1 - (\omega l/\pi)^2} \tag{B.10}$$

Substitution of (B.10) in (B.6) yields

$$\beta D^2\eta_1 + \beta\omega^2\eta_1 + \beta(k - \sin^2 \pi z/l)a_0 \sin \pi z/l + \beta^2(k - \sin^2 \pi z/l)\eta_1 = 0 \tag{B.11}$$

Neglect the term β^2 in the first order approximation. Then

$$D^2\eta_1 + \omega^2\eta_1 = - a_0(k - \sin^2 \pi z/l) \sin \pi z/l \tag{B.12}$$

Assume a solution in the form of Fourrier series. Thus

$$\eta_1 = \sum_1^n b_n \sin \pi z/l \tag{B.13}$$

Substitution of (B.13) in (B.12) yields

$$\sum_1^n b_n \left(-\frac{\pi^2 n^2}{l^2} + \omega^2\right) \sin \frac{\pi n z}{l} = - a_0(k - \sin^2 \pi z/l)\sin \pi z/l \tag{B.14}$$

To obtain the coefficient b_n multiply both sides by $\sin \pi z/l$ and integrate between zero and l. There follows:

$$\frac{l}{2} b_n \left(- \frac{\pi^2 n^2}{l} + \omega^2\right) = - a_0\left[\int_0^l k \sin \frac{\pi n z}{l} \sin \frac{\pi z}{l} dz - \int_0^l \sin \frac{\pi n z}{l} \sin^2 \frac{\pi z}{l} dz\right] \tag{B.15}$$

Hence, by putting $\pi z/l = x$

$$b_n = \frac{a_0}{\omega^2 - (\pi n/l)^2} \frac{2}{\pi}\left[k \int_0^{\pi} \sin nx \sin x dx - \int_0^{\pi} \sin nx \sin^2 x dx\right] \tag{B.16}$$

Since the first integral on the r.h.s. disappears for $n > 1$ the terms of (B.13) beyond the first one do not depend on k. The solution for η_1 can therefore be rewritten to read

$$\eta_1 = \frac{a_0}{\omega^2 - (\pi/l)^2}\left(k - \frac{3}{4}\right) \sin \pi z/l + \sum_2^n b_n \sin \pi n z/l \tag{B.17}$$

where b_n does not depend on k.

Since k is arbitrary we can reduce η_1 to a higher harmonic correction of η_0 by putting $k = 3/4$. The solution of (B.5) can then be rewritten in a more convenient form as follows:

$$\eta + \mu = \frac{a}{1 - (\omega l/\pi)^2}\left[\sin \pi z/l + \beta \sum_2^n \frac{C_n}{\omega_n^2} \sin \pi n z/l\right] \tag{B.18}$$

where C_n is a number and

$$\omega_n^2 = \omega^2 - (\pi n/l)^2 \tag{B.19}$$

Equation (B.18) shows that if β is small compared to unity the solution can be approximated by a simple sinusoid up to the first critical value of ω. That is,

$$\eta + \mu \approx \frac{a}{1 - (\omega l/\pi)^2} \sin \pi z/l \tag{B.20}$$

Putting $k = 3/4$ in (B.3) we have further

$$\omega^2 = \frac{P}{EI}\left(1 - 3/4 \frac{\Delta E}{E}\right) \tag{B.21}$$

or, since $\Delta E/E$ is small

$$\omega^2 = \frac{P}{(E + 3/4 \Delta E)I} \tag{B.22}$$

APPENDIX C

Parabolic Approximation in Semi-Elastic Column

The monotonic relation between stress and strain imposes the condition (1.8), Section 1 at $y = -h/2$, viz.,

$$|\eta''|_{max} < \frac{E_t}{G_t h} \tag{C.1}$$

or using nondimensional notation

$$|f''| < \frac{E_t}{G_t} \frac{l^2}{\pi^2 a h} \tag{C.2}$$

Let

$$E_t = k \frac{E_t + E_0}{2} \tag{C.3}$$

where k is a fraction, hence, since by definition

$$\alpha = 2G_t J a \pi^2 / (E_0 + E_t) I l^2 \tag{C.4}$$

$$|f''| < \frac{k}{\alpha} \frac{J}{I h} \tag{C.5}$$

On the other hand, solving (5.9), Section 5 for ϕ'' and putting $\zeta = \pi/2$ we have

$$|f''| = \frac{1 - \sqrt{1 - 4a\omega(1 + f)}}{2a} \tag{C.6}$$

Comparison of (C.5) to (C.6) gives

$$1 - \sqrt{1 - 4a\omega(1 + f)} \leq 2k \frac{J}{Ih} \tag{C.7}$$

Hence, solving for $1 + f$

$$1 + f \leq \frac{1 - \left(1 - 2k \frac{J}{Ih}\right)^2}{4\alpha\omega} \qquad (C.8)$$

For small values of f, E_t can be taken at the average stress level. For the case considered in Results, Section 5, E_o/E_t ranges from 1.21 for 20 hrs. to 1.42 to 60 hrs., hence on the average $k = 0.86$. For large values of f, E_t must be taken above the average stress level following the correction for the centroidal stress. Assuming a maximum decrease of 20% in E_t resulting from this correction we have $k_{min} = 0.78$.

Table C.1 below shows the comparison between values of $1 + f$ limited by relation (C.8) and those limited by the real roots of equation (5.9), Section 5, for a rectangular cross section.

TABLE C.1

ω	α	$1 + f$			Remarks
		Eq. (5.9)	Eq. (C.8)		
			$k = 0.86$	$k = 0.78$	
0.6	0.076	4.1	3.4		
0.65	0.052	4.5	4.5		
0.70	0.036	5.2	(6.2)	5.1	
0.73	0.029	6.0	(7.4)	6.1	$\omega + s > 1$

APPENDIX D

Error Due to Linear Approximation of the Isochronous Curves Below the Stress at the Centroid

If σ_c is the stress at the centroid we can write the stress-strain relations for the non-modified, isochronous curve $0\ C_0C_1A_1$ (see Figure 18a and b), as follows:

$$\sigma = \sigma_c + E_t\eta''y - G_t\eta''y^2 \qquad \text{for } -h_0 < y < 0 \qquad \text{(D.1)}$$

$$\sigma = \sigma_c + E_t\eta''y \qquad \text{for } m > y > 0 \qquad \text{(D.2)}$$

$$\sigma = \sigma_c + E_t\eta''m + E_0\eta''(y-m) \qquad \text{for } h_0 > y > m \qquad \text{(D.3)}$$

For simplicity the arc C_0C_1 has been approximated in (D.2) be the tangent at C_1 to the isochronous curve.

Inspection of Figure 18a shows that the error resulting from the substitution of $0\ C_0C_1$ by $0\ C_1$ is largest near the average stress, σ_0 and that it decreases toward point B_1 corresponding to the outer fiber. Thus, the relative error is greater for a rectangular section than for an I beam section since in the former the contribution of the inner fibers to the moment is greater.

If formulae (D.1) to (D.3) are used in the expression of moment for a rectangular cross section ($b \times 2h_0$) there follows:

$$\int\sigma y dA = b\int\sigma y dy = b\int_{-h_0}^{0}\sigma y dy + b\int_{0}^{m}\sigma y dy + b\int_{m}^{h_0}\sigma y dy = E_t\eta''I_0^{h_0} - G_t\eta''^2 J_0^{h_0}$$
$$+ bE_t\eta''\frac{m^3}{3} + bE_t\eta''m\left(\frac{h_0^2-m^2}{2}\right) + bE_0\eta''\left(\frac{h_0^3-m^3}{3}\right) - bE_0\eta''m\left(\frac{h_0^2-m^2}{2}\right) \qquad \text{(D.4)}$$

Expression (D.4) is to be compared to that of the moment due to simplified diagram OC_1A_1, viz.,

$$E_t \eta_*'' I_0^{h_0} - G_t \eta_*''^2 J_0^{h_0} + bE_0^* \eta_*'' \frac{h_0^3}{3} \tag{D.5}$$

where E_0^* is the slope of OC_1.

Inspection of formulae (D.4) and (D.5) shows that the error in deflection depends only on the discrepancy between the coefficients of η'' and η_*''. The difference between these coefficients is, if b is taken as unity,

$$(E_0 - E_0^*) \frac{h_0^3}{3} - (E_0 - E_t) \left[\frac{mh_0^2}{2} - \frac{m^3}{6}\right] \tag{D.6}$$

To evaluate the relative magnitude of this difference, form the ratio

$$\frac{(E_0 - E_0^*) \frac{h_0^3}{3} - (E_0 - E_t) \left(\frac{h_0^2}{2} - \frac{m^2}{6}\right) m}{(E_0^* + E_t) \frac{h_0^3}{3}} \tag{D.7}$$

where the denominator is the coefficient of η_*'' in (D.5).

From Figure 18a

$$\frac{E_0 - E_0^*}{E_0 - E_t} = \frac{C_0 D}{OL} = \frac{KK_1}{OK_1} = \frac{KK_1}{PK_1} \times \frac{PK_1}{OK_1} \tag{D.8}$$

But K_1K is the strain difference, relative to the centroid, at point C_0 located at a distance m from C_1. Likewise, PK_1 is the strain difference at point B_1, at a distance h_0 from C_1. Hence,

$$\frac{KK_1}{PK_1} = \frac{m}{h_0} \tag{D.9}$$

and

$$E_0 - E_0^* = (E_0 - E_t) \frac{m}{h_0} \frac{PK_1}{OK_1} \tag{D.10}$$

Substitution of (D.10) in (D.7) yields after simplification and division by common factor

$$\frac{(E_0 - E_t)\left[\frac{PK_1}{KK_1} - 1.5 + 0.5\left(\frac{m}{h_0}\right)^2\right]\frac{m}{h_0}}{E_t + E_0 - \left[E_0 - E_t\right]\frac{PK_1}{OK_1}\frac{m}{h_0}} \tag{D.11}$$

or, putting

$$\frac{E_0 - E_t}{E_0 + E_t} = k \tag{D.12}$$

and observing that for stress reversal at the outer fiber $PK_1 = OK_1$ we have for the relative difference of the coefficients of η'' and η''_* at the moment of stress reversal

$$-0.5k\,\frac{\frac{m}{h_0}\left[1-\left(\frac{m}{h_0}\right)^2\right]}{1 - k\,\frac{m}{h_0}} \tag{D.13}$$

We see that this difference is negative, i.e., the modified curve OC_1A_1 corresponds to smaller deflections and stiffer column.

In order to have an upper limit of the error (D.13) consider the isochronous curve at the 120th hour (see Figure 3). The computation of E_t gives a value of $k = 0.2$. Furthermore, assume

$$\frac{\sigma_c - \sigma_0}{\sigma_0} \approx \frac{KK_1}{OK_1} = \frac{m}{h_0} = 0.25 \tag{D.14}$$

Substitution of these values in (D.13) gives an error of 2.5%.

APPENDIX E

Approximate Solution of Nonlinear Differential Equation for Semi-Elastic Column

Rewrite equation (5.3), Section 5, as follows:

$$E_r I\eta''\left(1 + \frac{G_t J}{E_r I}\,\eta''\right) + P(\eta + \mu) = 0 \tag{E.1}$$

where

$$E_r = \frac{E_0 + E_t}{2} \tag{E.2}$$

Using relation between curvature and strain at the inner fiber ($y = -h/2$) we can write

$$\frac{G_t J}{E_r I}\,\eta'' = \frac{2G_t}{E_r}\,\frac{J}{Ih}\,\eta''\,\frac{h}{2} = -\,\beta\,\frac{2G_t}{E_r}\,\Delta\epsilon_A \tag{E.3}$$

where

$$\frac{J}{Ih} = \beta \tag{E.4}$$

Also, if E_A is the tangent modulus at $y = -h/2$

$$-\Delta\epsilon_A = \frac{E_A - E_t}{2G_t} \tag{E.5}$$

Substitution of (E.3) and (E.5) in (E.1) yields

$$E_r I\eta''\left(1 + \beta\,\frac{E_A - E_t}{E_r}\right)\eta'' + P(\eta + \mu) = 0 \tag{E.6}$$

The difference $E_A - E_t$ in equation (E.6) varies with z in the same way as η''. That is, it is maximum at the midlength, where $z = l/2$ and nil at both ends of the column. If the second term in brackets is small

compared to unity we can write as a first approximation

$$E_A - E_t = \Delta E \sin \frac{\pi z}{l} \tag{E.7}$$

ΔE is the value of the above difference at the midlength of column.

Substitution of (E.7) in (E.6) and rearrangement of terms yields

$$\eta'' + \frac{P}{E_r I\left(1 + \beta \frac{\Delta E}{E_r} \sin \frac{\pi z}{l}\right)} (\eta + \mu) = 0 \tag{E.8}$$

Equation (E.8) is similar in nature to equation (B.1), Appendix B. Proceeding as explained there we find

$$\eta = \frac{\mu}{\frac{P_r}{P} + \frac{\Delta P}{P} - 1} \tag{E.9}$$

where

$$\Delta P = \beta' \pi^2 \Delta E I / l^2 , \tag{E.10}$$

$$P_r = \pi^2 E_r I / l^2 , \tag{E.11}$$

and

$$\beta' = 0.85 \beta \tag{E.12}$$

The value of ΔP is not given a priori. However, it can be found if it is recalled that

$$\Delta \epsilon = - \eta'' \frac{h}{2} = \frac{\left(\frac{\pi}{l}\right)^2 \frac{ah}{2}}{\frac{P_r}{P} + \frac{\Delta P}{P} - 1} \tag{E.13}$$

and

$$- \Delta \epsilon = \frac{\Delta E}{2G_t} = \frac{\Delta P l^2}{1.70 \beta \pi^2 I G_t} \tag{E.14}$$

Combining (E.13) and (E.14) there follows:

$$-\Delta P = \frac{(\pi/l)^2 \frac{ah}{2} P(\delta P)}{P_r - P + \Delta P} \qquad \text{(E.15)}$$

where for brevity

$$(\delta P) = 1.70\beta \frac{\pi^2 G_t I}{l^2} \qquad \text{(E.16)}$$

Solving (E.15) for ΔP and noticing that only the smaller of the two roots is the solution to our problem we have

$$\Delta P = \frac{P_r - P - \sqrt{(P_r - P)^2 - 2ahP(\delta P)(\pi/l)^2}}{2} \qquad \text{(E.17)}$$

Substitution of (E.17) in (E.9) yields the value for the deflection a_t as follows:

$$a_t = \frac{2}{\left(\frac{P_r}{P} - 1\right) + \sqrt{\left(\frac{P_r}{P} - 1\right)^2 - 3.4\beta \left(\frac{\pi}{l}\right)^4 \frac{ahG_t I}{P}}} \qquad \text{(E.18)}$$

or using nondimensional notations

$$f = \frac{2}{\left(\frac{1}{\omega} - 1\right) + \sqrt{\left(\frac{1}{\omega} - 1\right)^2 - 3.4 \frac{\alpha}{\omega}}} \qquad \text{(E.19)}$$

Table E.1 shows the comparison between (E.19) and the solution obtained by means of the differential analyzer (marked as D. A. in the Table). As expected, the approximate solution gives lower values than the exact one. The discrepancy increases as α becomes larger.

TABLE E.1

COMPARISON BETWEEN APPROXIMATE (Appr.)
AND EXACT (D.A.) SOLUTIONS OF DEFLECTION.

ω	α 10^{-2}	f		Error %
		Appr.	D.A.	
0.8	0.5	4.43	4.50	1.5
	1.0	5.05	5.20	3.0
	1.3	6.00	6.20	3.3
0.73	0.5	2.82	2.85	1.0
	1.0	3.00	3.05	1.6
	2.0	3.45	3.50	1.4
	2.5	3.92	4.00	2.0
	2.9	4.85	5.30	8.5
0.6	1.0	1.55	1.60	3.0
	2.0	1.60	1.65	3.0
	4.0	1.73	1.80	3.9
	6.2	2.04	2.15	5.1

APPENDIX F

Approximate Solution of the Equation $\eta'' + \omega^2(\eta + \cos z) + \alpha\eta'^2 = 0$ **by the Method of Linstead and Liapounoff.***

Expand η and ω^2 in power series of α

$$\eta = \eta_0 + \alpha\eta_1 + \alpha^2\eta_2 + \cdots$$
$$\omega^2 = \omega_0^2 + \alpha C_1 + \alpha^2 C_2 + \cdots \qquad \text{(F.1)}$$

Making the appropriate substitution and collecting coefficients of like powers of α gives

$$\eta_0'' + \omega_0^2\eta_0 = -\omega_0^2\cos z$$
$$\eta_1'' + \omega_0^2\eta_1 = -C_1(\eta_0 + \cos z) - \eta_0'^2$$
$$\eta_2'' + \omega_0^2\eta_2 = -C_2(\eta_0 + \cos z) - C_1\eta_1 - 2\eta_0''\eta_1'' \qquad \text{(F.2)}$$
$$+ \cdots \qquad + \cdots$$

The solution of equations (F.2) has to satisfy the following boundary conditions:

$$\eta_{\pm\frac{\pi}{2}} = \eta'_{\pm\frac{\pi}{2}} = 0 \qquad \text{(F.3)}$$

It can be shown that (F.3) requires that C_1 and C_2 be zero. The value of η takes the form

---

* L. A. Pipes, Applied Mathematics for Engineers and Physicists, First Edition, McGraw-Hill, 1946, pp. 587-595.

$$\eta = -\frac{\omega^2}{T}\cos z - \alpha\frac{\omega^4}{2T^2T_2}\left(\frac{T_2}{\omega^2} + \cos 2z + \frac{4\cos\omega z}{\omega^2\cos(\omega\pi/2)}\right) - \alpha^2\frac{2\omega^6}{T^3T_2}$$

$$\left[\frac{\cos z}{T} + \frac{\cos 3z}{T_3} + \frac{1}{\cos\frac{\omega\pi}{2}}\left(\frac{\cos\omega - 1}{2\omega - 1} - \frac{\cos\omega + 1}{2\omega + 1} - \frac{\omega\tan\omega\pi/2}{T_{\frac{1}{2}}}\cos\omega z\right)\right] + \cdots$$

(F.4)

where $T = -1 + \omega^2$ and $T_n = -n^2 + \omega^2$. For $\omega^2 = 0.6$ values of η are obtained as follows:

α	η	
	by (F.4)	by differential analyzer
.01	1.53	1.60
.02	1.56	1.65
.04	1.62	1.80
.062	1.72	2.15

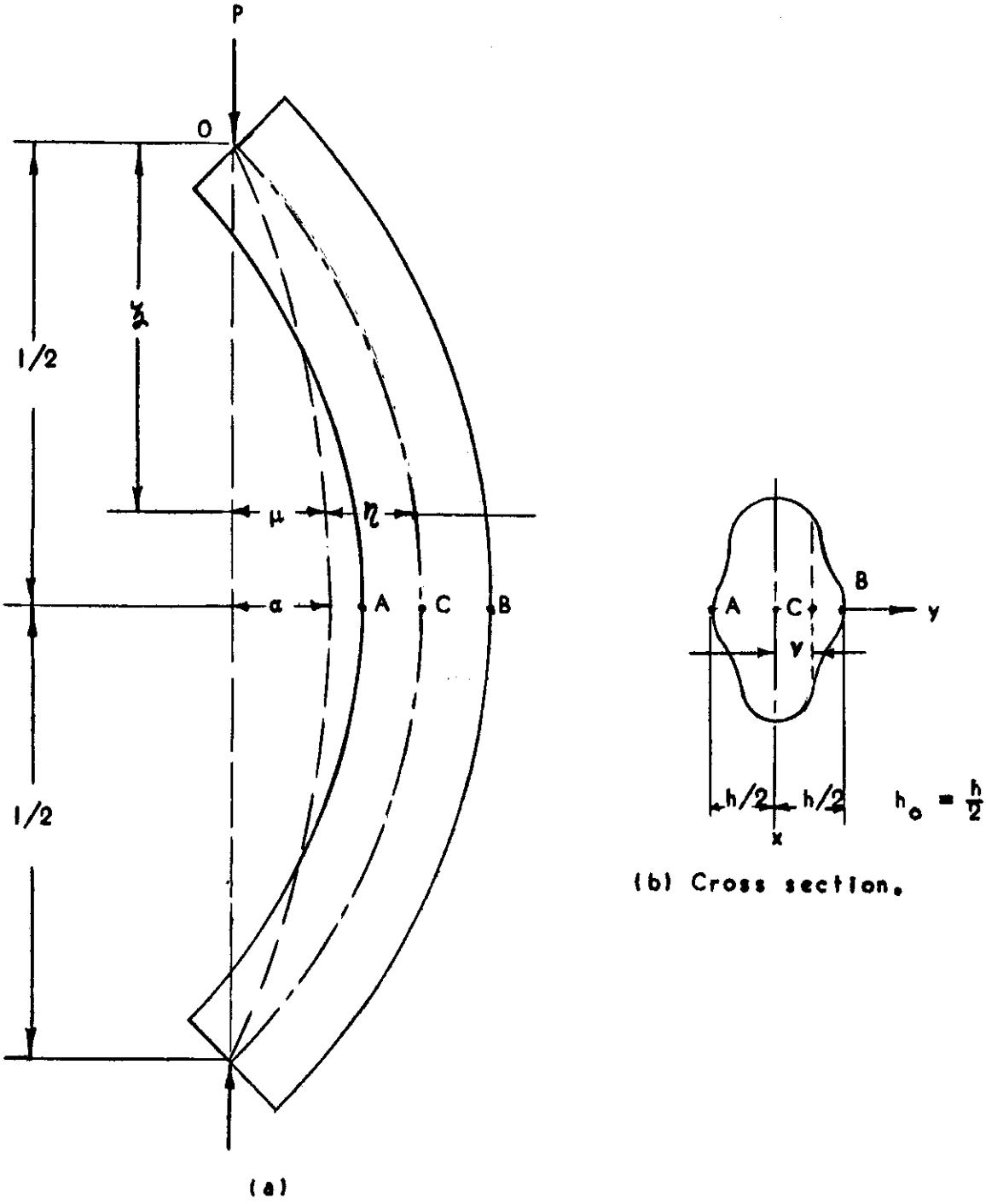

Figure 1. Dimensions and notations referring to column.

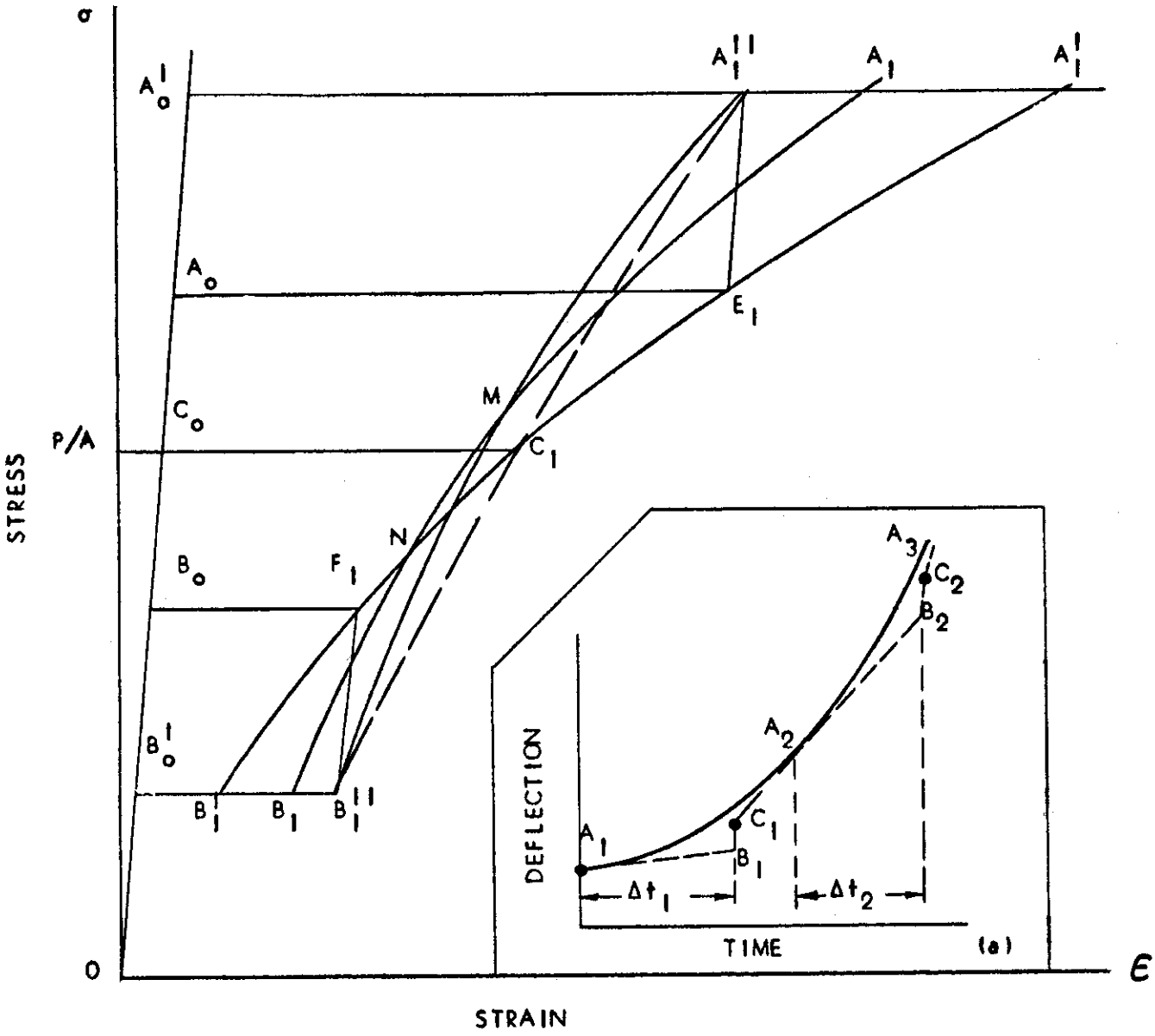

Figure 2. Criteria for upper and lower bound.
Cut (a) Real and upper bound deflections.

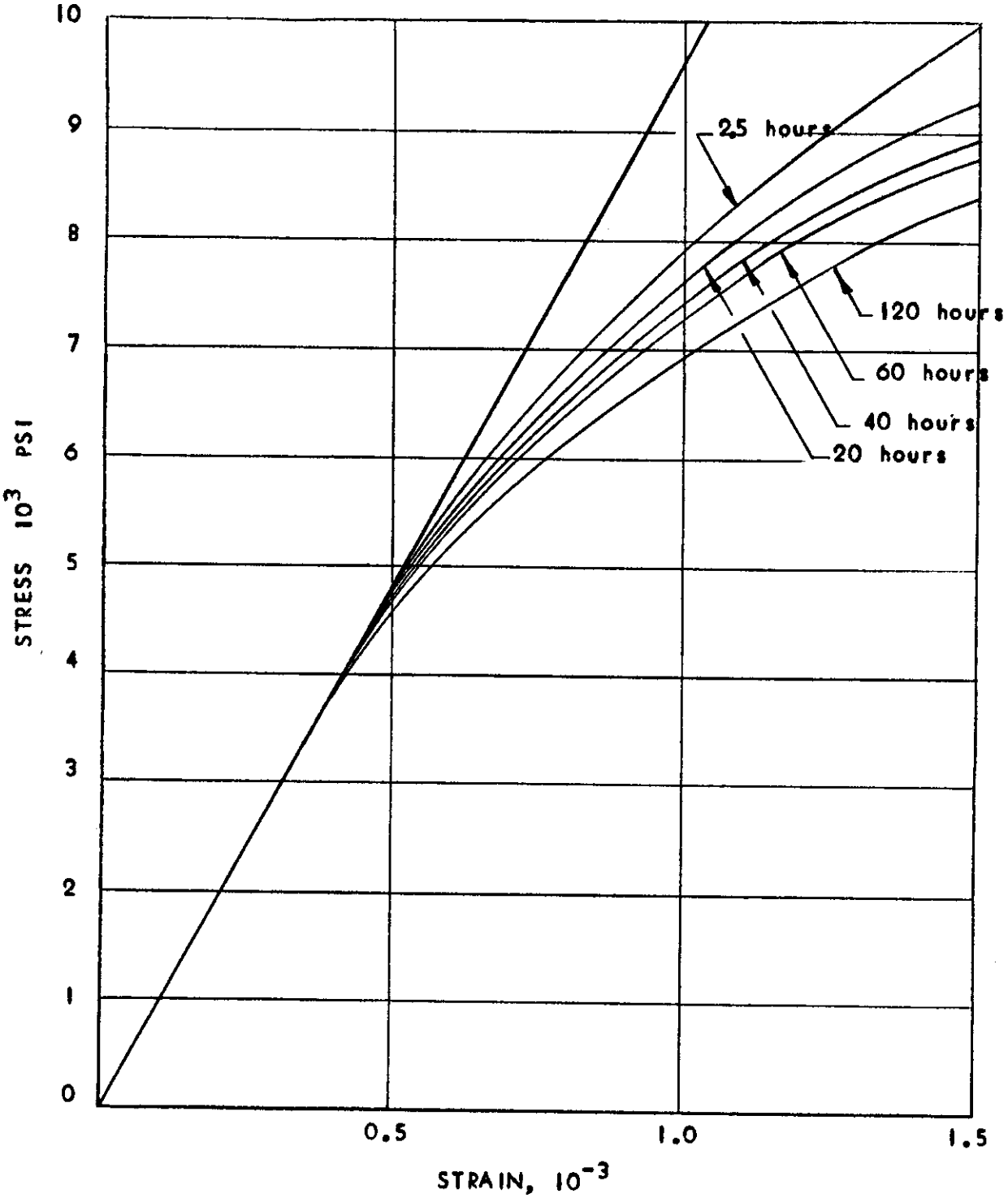

Figure 3. Isochronous curves at 350° F for 24S stabilized Aluminum Alloy.

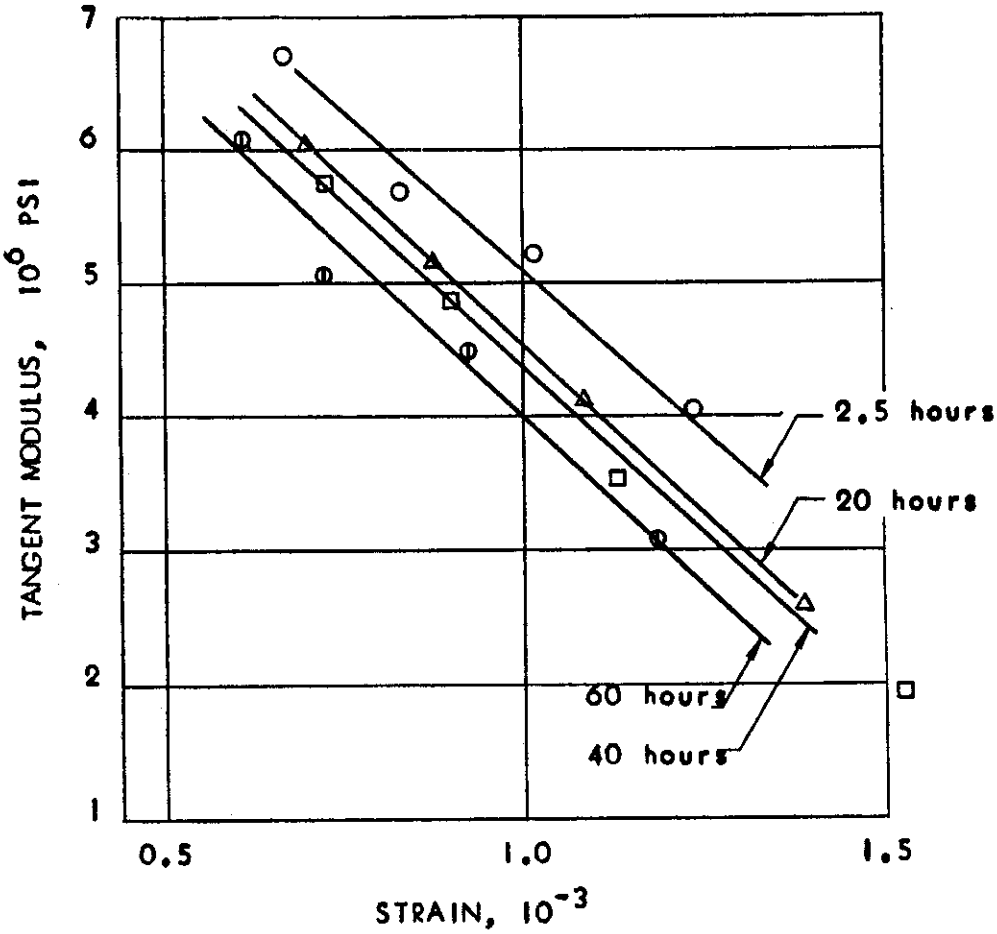

Figure 4. Validity of parabolic approximation. Plot of tangent modulus, E vs. strain from isochronous curves, Figure 3.

Figure 5. Time deflection curves for the lower bound.
Stabilized 24S Aluminum Alloy at 350° F.
l/r = 81.4 . Solid lines P = 870 lbs., or $P/P_o = 0.485$
Chained lines P = 840 lbs., or $P/P_o = 0.470$
Dashed lines - experimental
Various initial eccentricities, α as indicated, P_o = 1800 lbs.

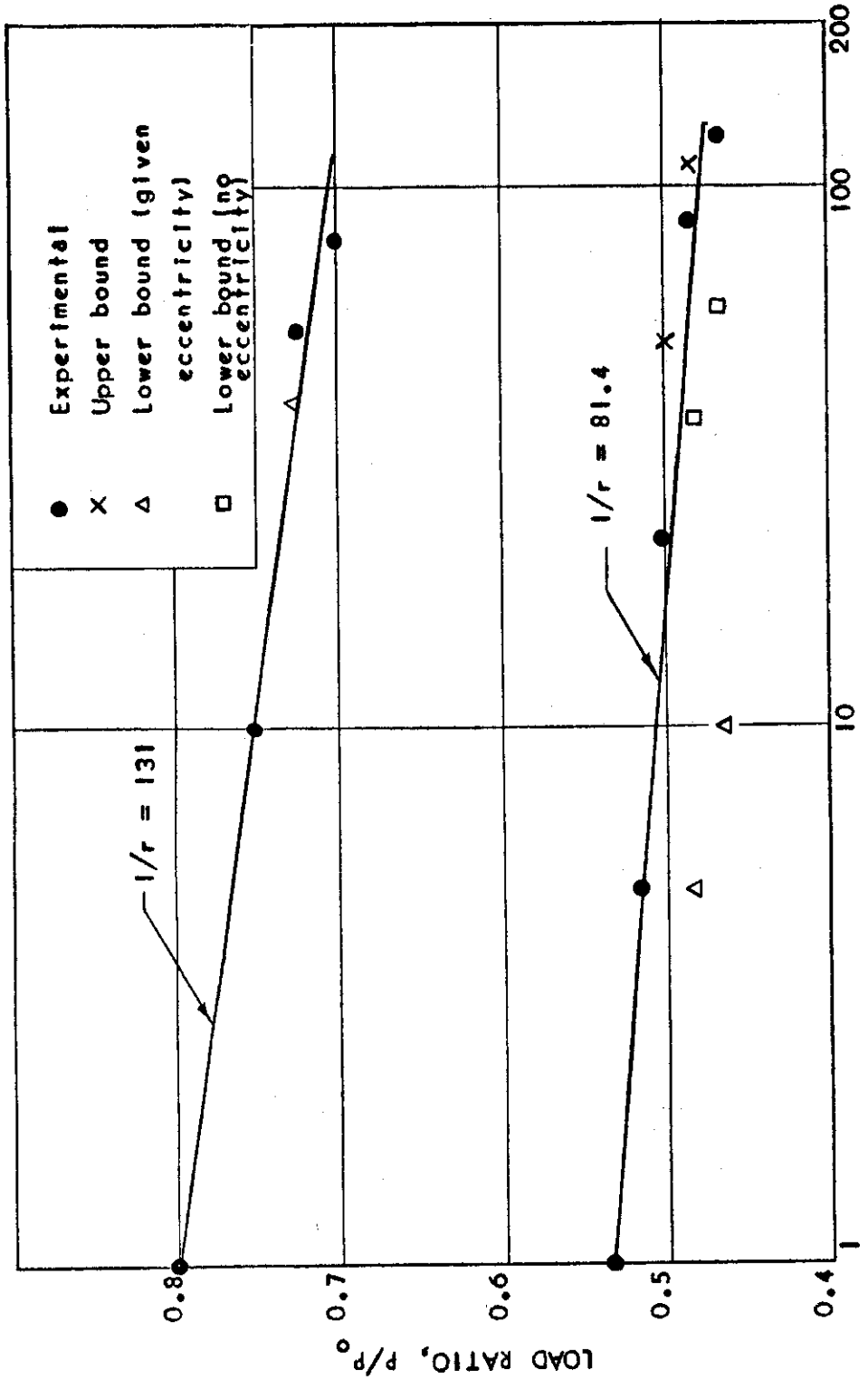

Figure 6. Load ratio P/P_o vs. time for total deflection equal to core radius, or $\omega + e = 1.0$.

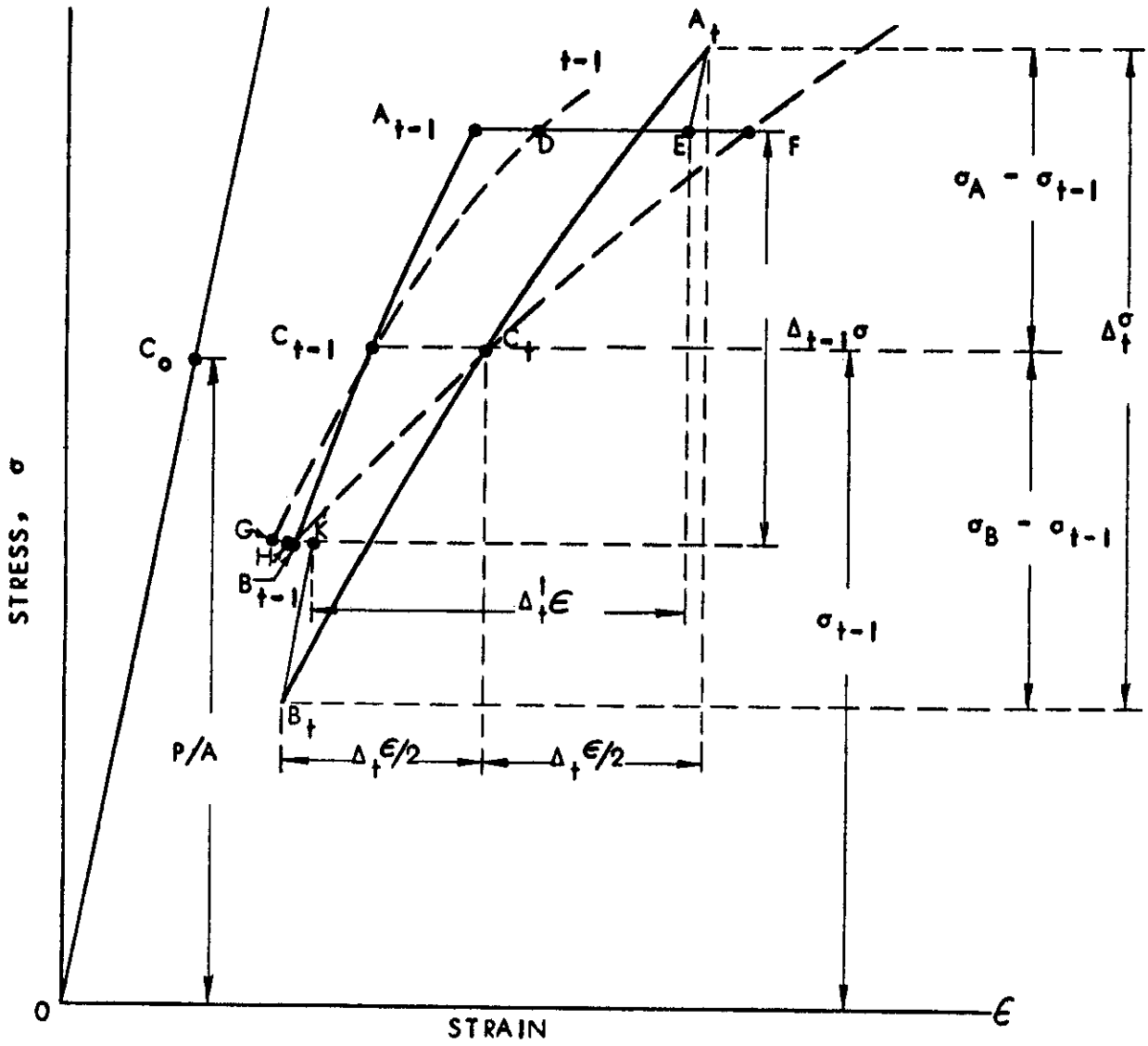

Figure 7. Recurrent procedure for the upper bound.

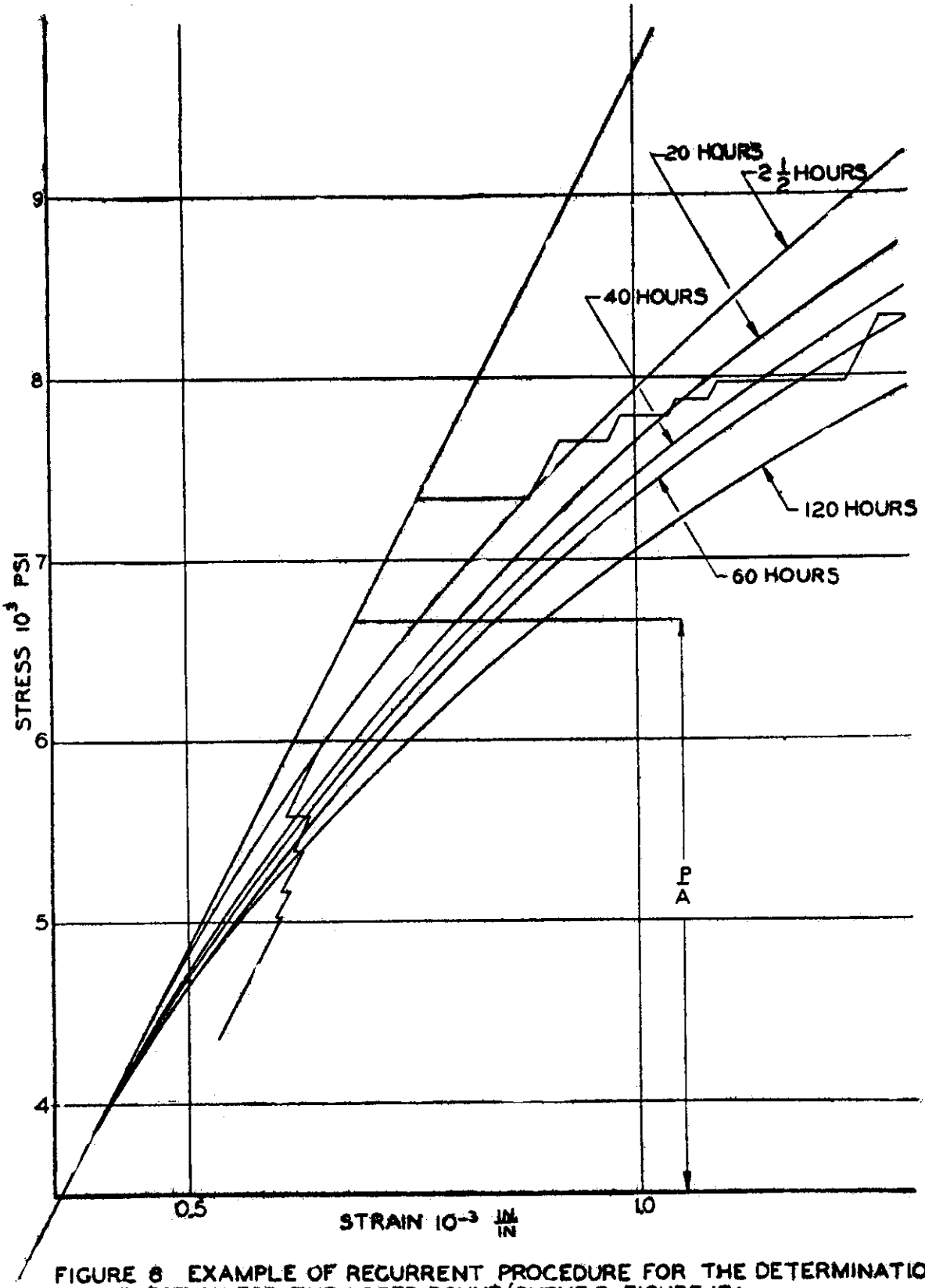

FIGURE 8 EXAMPLE OF RECURRENT PROCEDURE FOR THE DETERMINATION OF DEFLECTION FOR THE UPPER BOUND (CURVE B, FIGURE 10)

Figure 9. Time deflection curves for the upper bound Stabilized 24S Aluminum Alloy at 350° F. Various loads and eccentricities. Dashed lines -- experimental. P_o = 1800 lbs.

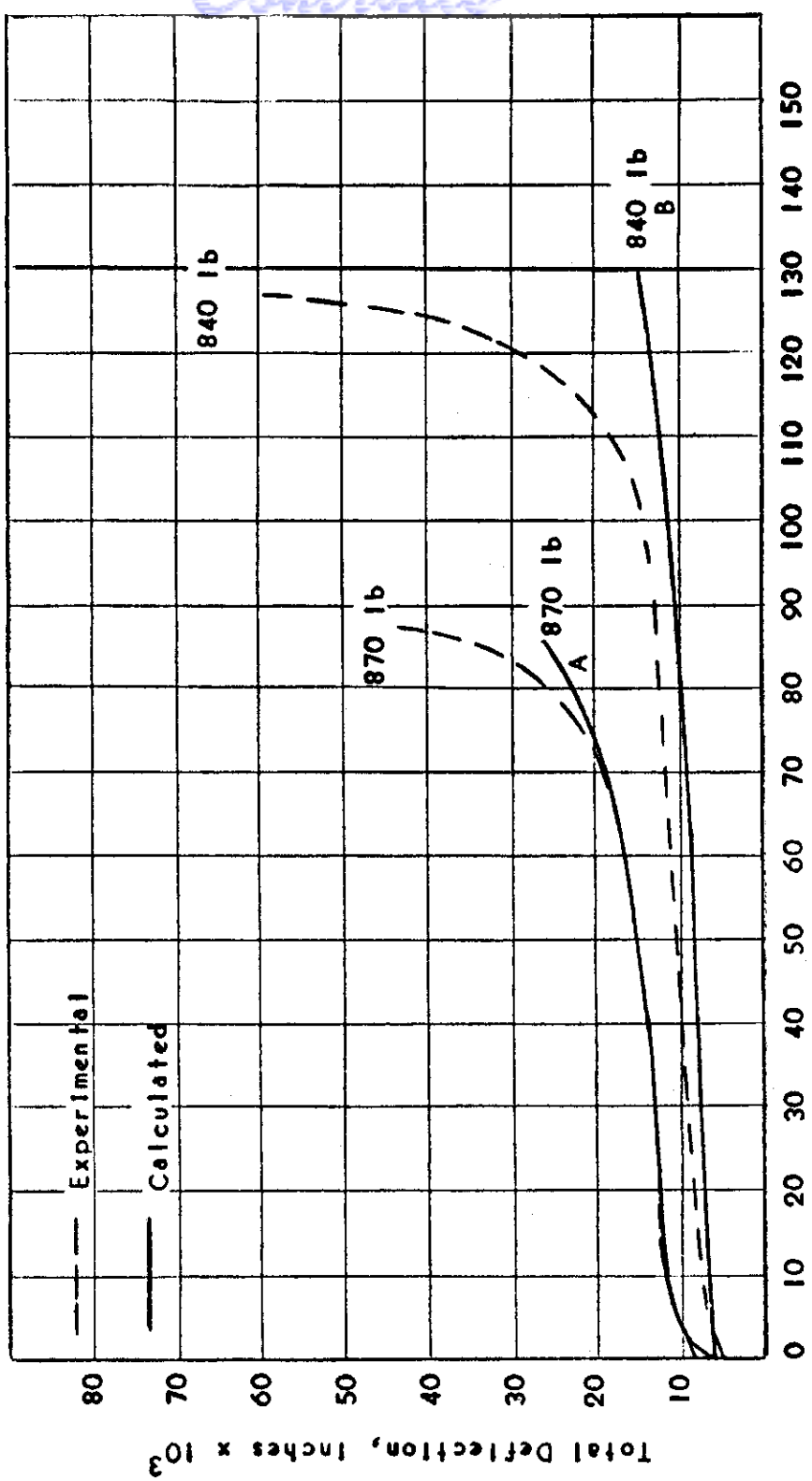

Figure 10. Time-deflection curves for upper bound. Computed deflections adjusted to match experimental deflections at 2.5 hrs. Stabilized 24S Aluminum Alloy, $^{1}/_{r} = 81.4$, 350°F.

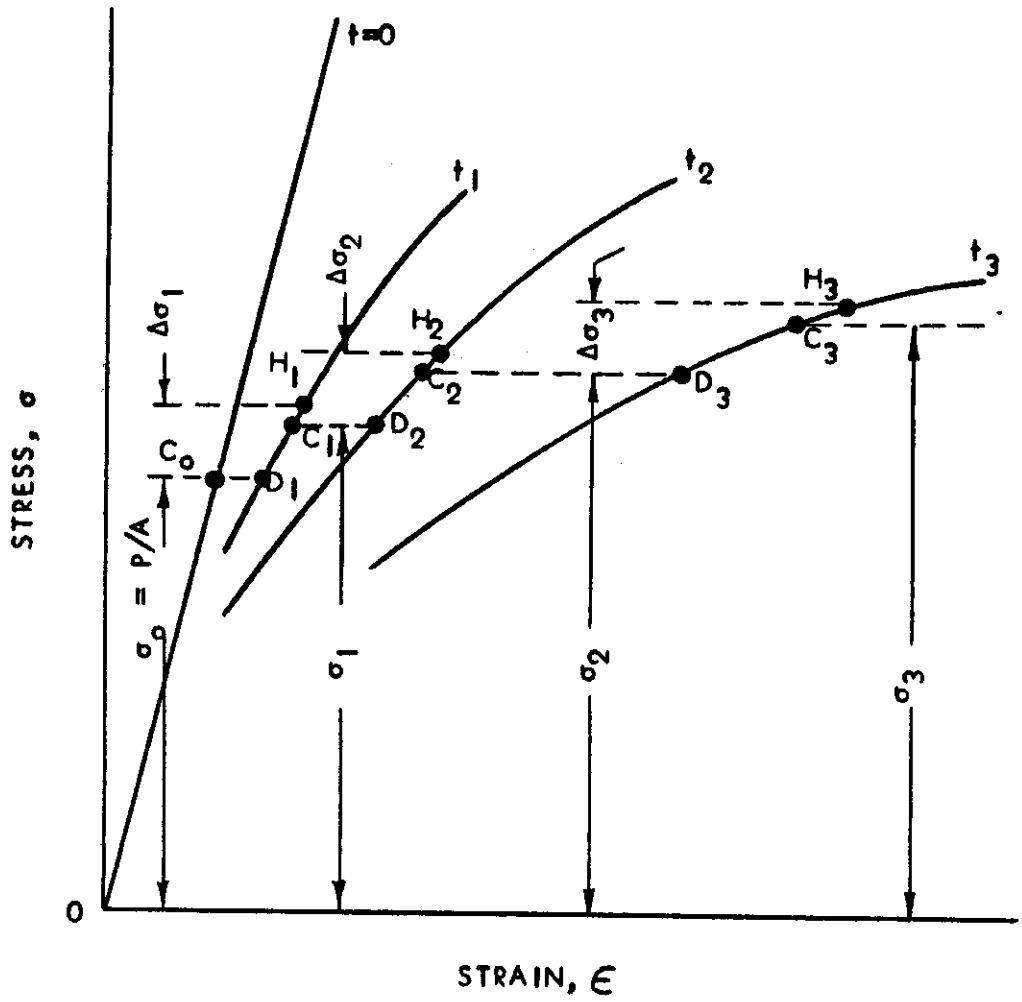

Figure 11. Correction for the stress at the centroid.

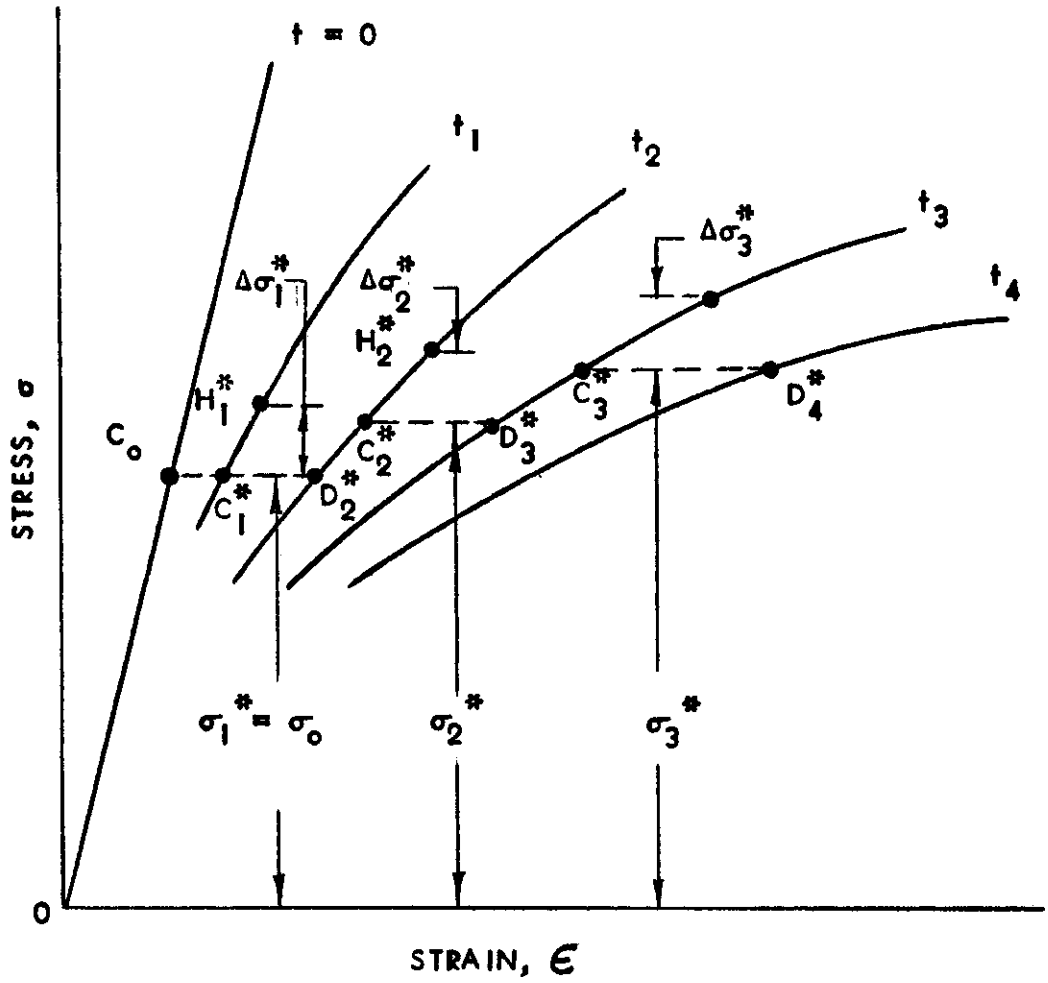

Figure 12. Approximate correction for the stress at the centroid.

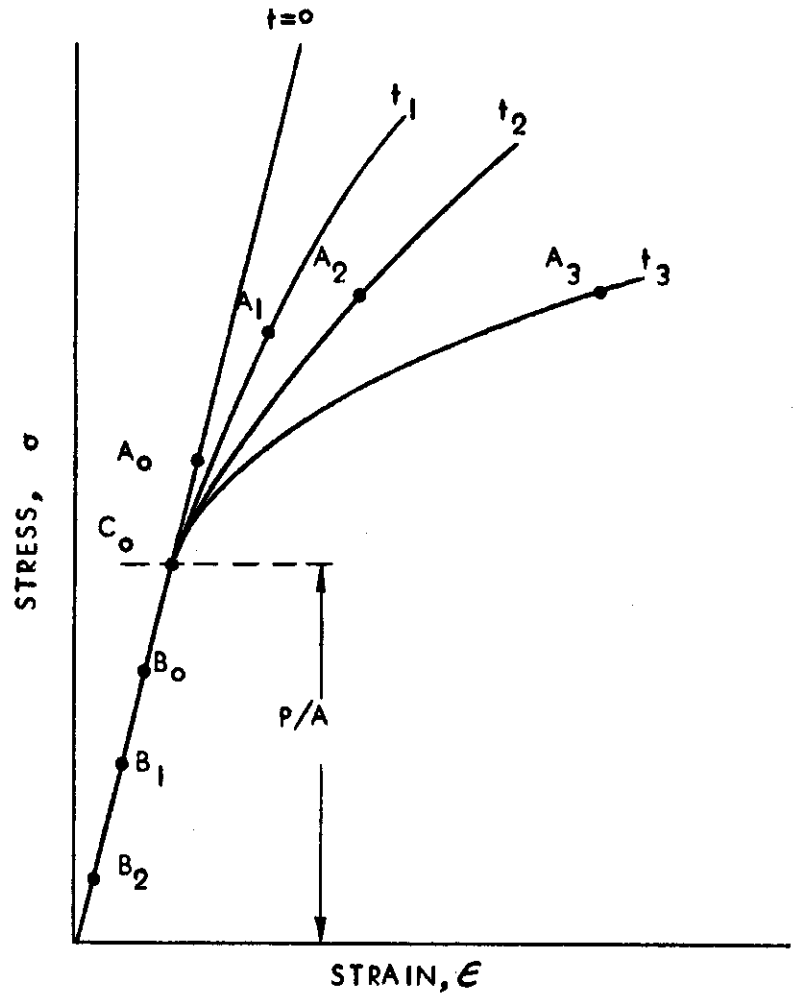

Figure 13. Semi-elastic column.

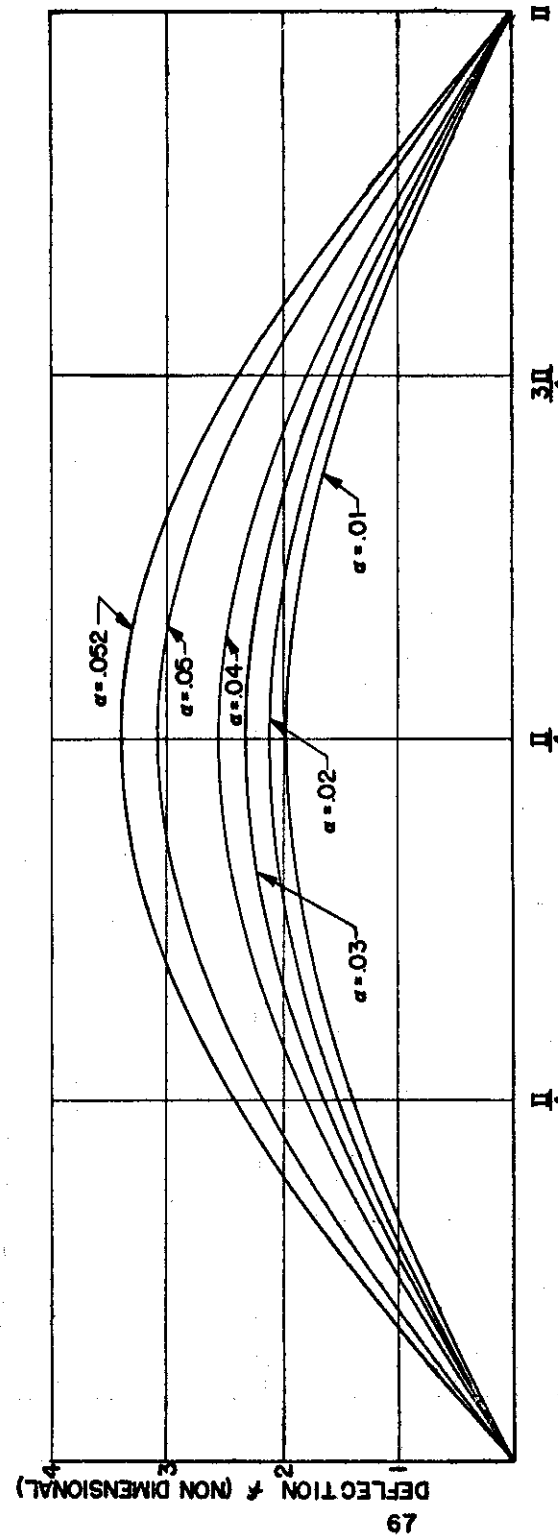

FIGURE 14 TYPICAL DEFLECTION CURVES OBTAINED BY MEANS OF DIFFERENTIAL ANALYZER FOR ω =0.65 AND VARIABLE PARAMETER α

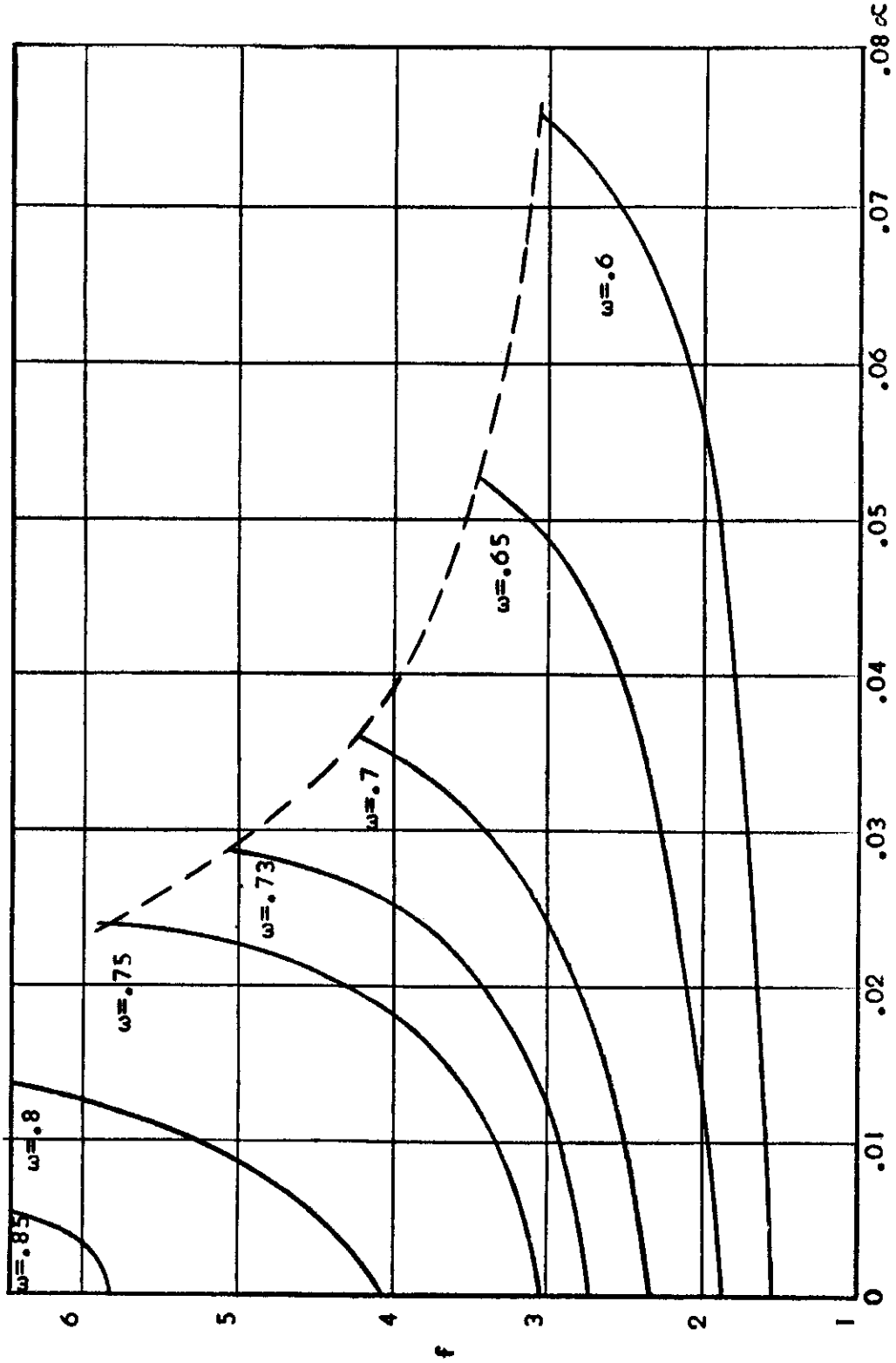

Figure 15. Maximum deflection, f as a function of parameters ω and α determined by means of differential analyzer.

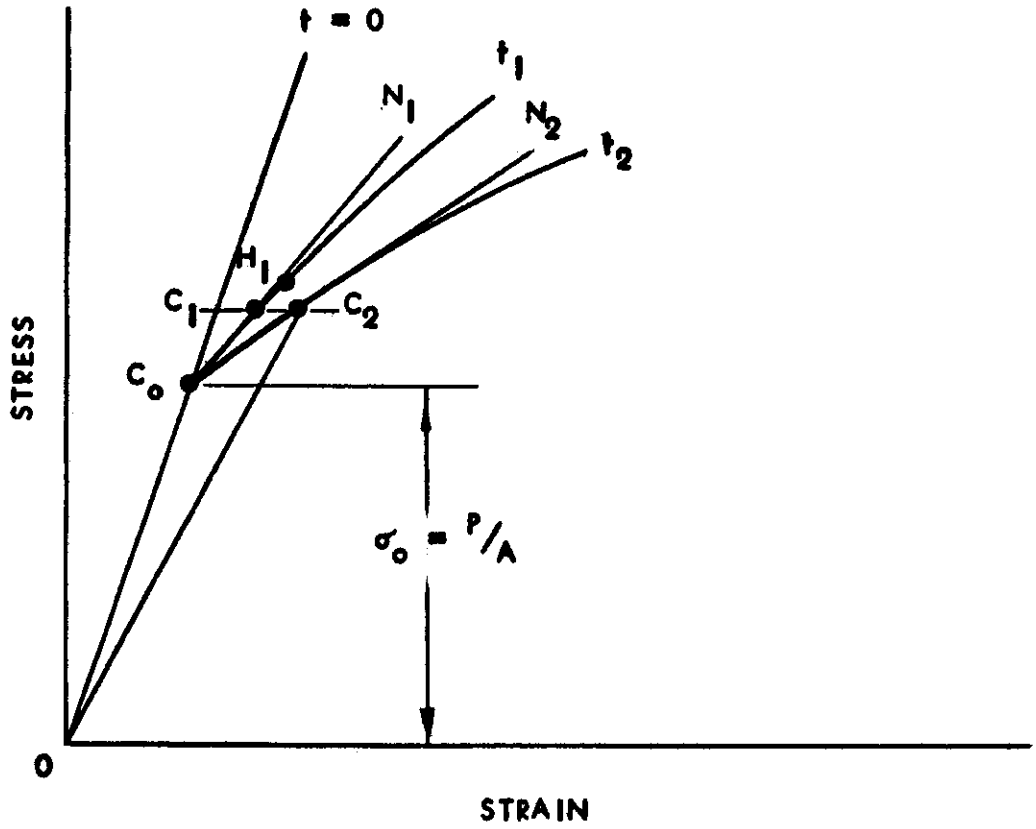

Figure 16. Approximate procedure for correcting the stress at the centroid in a semi-elastic column.

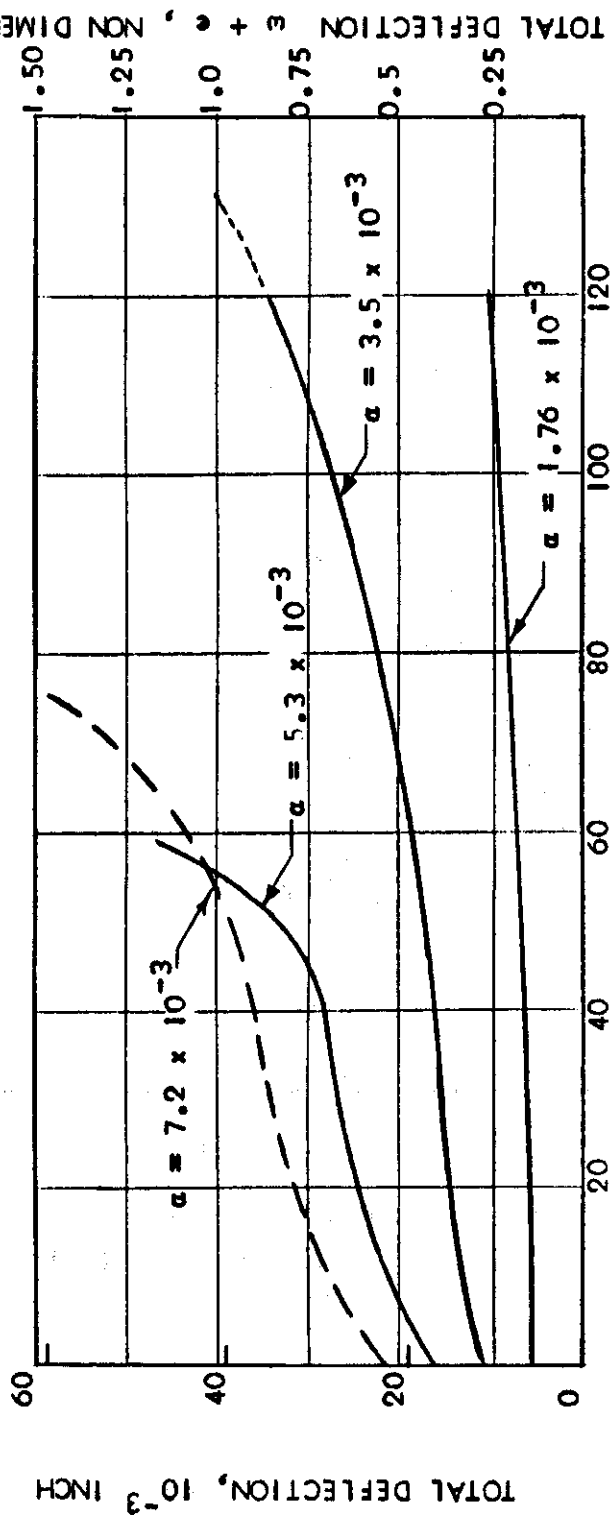

Figure 17. Time deflection curves for semi elastic columns.
P = 503 lb., l/r = 131 24S Aluminum Alloy at 350° F.
Dashed line - experimental Load ratio - $\frac{P}{P_o}$ = .72
Solid line - calculated

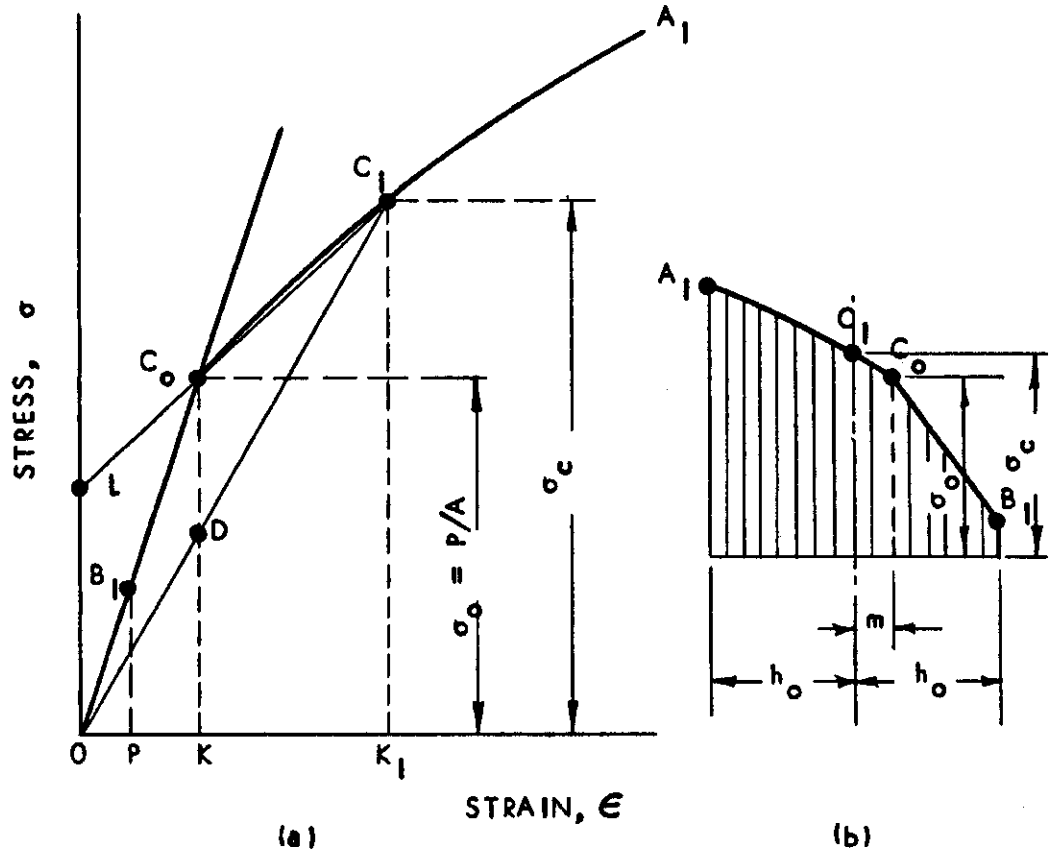

Figure 18. Computation of error in approximate procedure for correcting the stress at the centroid.

(a) stress strain diagram.

(b) stress distribution in the cross section.